

Dissociation cross sections of large-momentum charmonia with light mesons in hadronic matter

Yi-Hao Pan¹, Wen-Hao Shi¹, Xiao-Ming Xu¹ and H. J. Weber²

¹Department of Physics, Shanghai University, Baoshan, Shanghai 200444, China

²Department of Physics, University of Virginia, Charlottesville, VA 22904, USA

Abstract

Momenta of charmonia created in Pb-Pb collisions at the CERN Large Hadron Collider are so large that three or more mesons may be produced when the charmonia collide with light mesons in hadronic matter. We study the meson-charmonium collision in a mechanism where the collision produces two quarks and two anti-quarks; the charm quark then fragments into charmed mesons, and the other three constituents as well as quarks and antiquarks created from vacuum give rise to two or more mesons. The absolute square of the transition amplitude for the production of two quarks and two antiquarks is derived from the S -matrix element, and cross-section formulas are derived from the absolute square of the transition amplitude and charm-quark fragmentation functions. With a temperature-dependent quark potential, we calculate unpolarized cross sections for inclusive D^+ , D^0 , D_s^+ , or D^{*+} production in scattering of charmonia by π , ρ , K , or K^* mesons. At low center-of-mass energies of the charmonium and the light meson, the cross sections are very small. At high energies the cross sections have obvious temperature dependence, and are comparable to peak cross sections of two-to-two meson-charmonium reactions.

Keywords: Charmonium dissociation, Relativistic constituent quark potential model

PACS: 13.75.Lb; 12.39.Jh; 12.39.Pn

1. Introduction

Plenty of efforts with quantum chromodynamics (QCD) and effective field theories have been devoted to exploring strong interactions of charmonia with light hadrons. Four main approaches involved in the study are the short-distance approach, the effective meson approach, the quark-interchange approach, and QCD sum rules. In the short-distance approach, methods in perturbative QCD, for example, the operator product expansion, were applied to charmonia of small sizes [1–3]. In the effective meson approach, effective meson Lagrangians with different symmetries and Feynman diagrams with various vertex functions have been used to get millibarn-scale cross sections for meson-charmonium reactions [4–14]. Recently, $\pi J/\psi$, $\rho\eta_c$, and $D\bar{D}^*$ ($D^*\bar{D}$) reactions have been put together to form coupled channels. The corresponding scattering amplitude derived in $SU(4)$ chiral perturbation theory is unitarized [12–14], and cross sections obtained for $\pi J/\psi$ dissociation are different from those given in Refs. [4–11]. In the quark-interchange approach, charmonium dissociation in collisions with light mesons is caused by quark interchange [15] between the charmonium and the meson. The dissociation has been studied in the Born approximation with quark potentials which reproduce spectroscopic data and provide mesonic quark-antiquark wave functions [16–21]. In the QCD sum rules, $\pi J/\psi$ dissociation cross sections were obtained from the general vacuum-pion correlation function with the currents of J/ψ and of charmed mesons in the soft-pion limit [22].

The studies reported in Refs. [1–14, 16–18, 22] concentrate on charmonium dissociation in vacuum. In hadronic matter the dissociation is different [23]. From perturbative QCD and lattice QCD, a temperature-dependent quark potential was derived in Refs. [19, 24]. This potential leads to temperature dependence of meson masses, mesonic quark-antiquark relative-motion wave functions, and dissociation cross sections [19–21]. Adopting temperature dependence in meson masses and two-meson Green functions in the coupled-channel unitary approach, temperature-dependent cross sections for J/ψ scattering by light mesons have been obtained in Ref. [25].

For Pb-Pb collisions at the center-of-mass energy per nucleon-nucleon pair $\sqrt{s_{NN}} =$

5.02 TeV at the CERN Large Hadron Collider, the prompt- J/ψ transverse momentum measured by the CMS Collaboration [26] and the ATLAS Collaboration [27] goes up to 50 GeV/ c . J/ψ mesons with such large transverse momenta may be broken up due to collisions with light mesons in hadronic matter, and three or more mesons can be produced. Since the reactions studied in Refs. [4–14, 16–22, 25] were limited to two-to-two meson-charmonium reactions, a mechanism for large-momentum charmonium dissociation is proposed in Ref. [28] to study the production of three or more mesons in pion-charmonium collisions. In this mechanism a collision between a light meson and a charmonium produces quarks and antiquarks first, the charm quark then fragments into charmed hadrons, and finally three or more mesons are produced. Besides pions, ρ mesons, kaons, vector kaons, and so on in hadronic matter also induce charmonium dissociation. This motivates studying the production of three or more mesons in the dissociation of large-momentum charmonia in collisions with light mesons in the present work.

This paper is organized as follows. In the next section we derive cross-section formulas for dissociation of large-momentum charmonia in collisions with light mesons. Numerical results and relevant discussions are presented in Section 3. A summary is in the last section.

2. Formalism

We obtain the cross section for $A(q_1\bar{q}_2) + B(c\bar{c}) \rightarrow q_1 + \bar{q}_2 + c + \bar{c} \rightarrow H_c + X$ from the cross section for $A + B \rightarrow q_1 + \bar{q}_2 + c + \bar{c}$ and the fragmentation function for $c \rightarrow H_c$, where H_c represents a hadron that contains the charm quark. The fragmentation of the charm quark into hadrons is related to quark-antiquark pairs created from the color field around the charm quark, which is that scenario of Feynman and Field [29]. The charm quark may combine the antiquark of a quark-antiquark pair to form meson H_c . Two quark-antiquark pairs may also form another H_c . All possible ways to form meson H_c are accounted for by the $c \rightarrow H_c$ fragmentation function. Hence, only one H_c symbol is in $A(q_1\bar{q}_2) + B(c\bar{c}) \rightarrow q_1 + \bar{q}_2 + c + \bar{c} \rightarrow H_c + X$. Unused quarks and antiquarks combine q_1, \bar{q}_2 , and \bar{c} to form two or more mesons. The symbol X indicates the two or more mesons that

do not include meson H_c . We first derive cross-section formulas for $A + B \rightarrow q_1 + \bar{q}_2 + c + \bar{c}$. Let E_i be the total energy of mesons A and B , and E_f be the one of constituents q_1, \bar{q}_2, c , and \bar{c} . The S -matrix element for $A + B \rightarrow q_1 + \bar{q}_2 + c + \bar{c}$ is

$$\begin{aligned} S_{fi} = & \delta_{fi} - 2\pi i \delta(E_f - E_i) (\langle q_1, \bar{q}_2, c, \bar{c} | V_{q_1 \bar{c}} | A, B \rangle + \langle q_1, \bar{q}_2, c, \bar{c} | V_{\bar{q}_2 c} | A, B \rangle \\ & + \langle q_1, \bar{q}_2, c, \bar{c} | V_{q_1 c} | A, B \rangle + \langle q_1, \bar{q}_2, c, \bar{c} | V_{\bar{q}_2 \bar{c}} | A, B \rangle), \end{aligned} \quad (1)$$

where V_{ab} is the potential between constituents a and b . Let \vec{r}_{ab} be the relative coordinate of a and b , and denote the momentum and the position vector of meson A (B) by \vec{P}_A (\vec{P}_B) and \vec{R}_A (\vec{R}_B), respectively. The wave function $|A, B\rangle$ of A and B is

$$\psi_{AB} = \frac{e^{i\vec{P}_A \cdot \vec{R}_A}}{\sqrt{V}} \psi_A(\vec{r}_{q_1 \bar{q}_2}) \frac{e^{i\vec{P}_B \cdot \vec{R}_B}}{\sqrt{V}} \psi_B(\vec{r}_{c \bar{c}}), \quad (2)$$

where every meson wave function is normalized in the volume V , and ψ_A (ψ_B) is a wave function of color, flavor, spin, and relative motion of the quark and the antiquark in meson A (B). Let \vec{p}'_{q_1} ($\vec{p}'_{\bar{q}_2}$, \vec{p}'_c , $\vec{p}'_{\bar{c}}$) and \vec{r}_{q_1} ($\vec{r}_{\bar{q}_2}$, \vec{r}_c , $\vec{r}_{\bar{c}}$) denote the momentum and the position vector of q_1 (\bar{q}_2 , c , \bar{c}), respectively. The wave function $|q_1, \bar{q}_2, c, \bar{c}\rangle$ of q_1, \bar{q}_2, c , and \bar{c} is

$$\psi_{q_1 \bar{q}_2 c \bar{c}} = \frac{e^{i\vec{p}'_{q_1} \cdot \vec{r}_{q_1}}}{\sqrt{V}} \frac{e^{i\vec{p}'_{\bar{q}_2} \cdot \vec{r}_{\bar{q}_2}}}{\sqrt{V}} \frac{e^{i\vec{p}'_c \cdot \vec{r}_c}}{\sqrt{V}} \frac{e^{i\vec{p}'_{\bar{c}} \cdot \vec{r}_{\bar{c}}}}{\sqrt{V}} \varphi_{q_1 \bar{q}_2 c \bar{c} \text{color}} \varphi_{q_1 \bar{q}_2 c \bar{c} \text{flavor}} \varphi_{q_1 \bar{q}_2 c \bar{c} \text{spin}}, \quad (3)$$

where $\varphi_{q_1 \bar{q}_2 c \bar{c} \text{color}}$, $\varphi_{q_1 \bar{q}_2 c \bar{c} \text{flavor}}$, and $\varphi_{q_1 \bar{q}_2 c \bar{c} \text{spin}}$ are the color wave function, the flavor wave function, and the spin wave function of q_1, \bar{q}_2, c , and \bar{c} , respectively. Using the wave functions, we get

$$\begin{aligned} \langle q_1, \bar{q}_2, c, \bar{c} | V_{ab} | A, B \rangle = & \int d\vec{r}_{q_1} d\vec{r}_{\bar{q}_2} d\vec{r}_c d\vec{r}_{\bar{c}} \psi_{q_1 \bar{q}_2 c \bar{c}}^+ V_{ab} \psi_{AB} \\ = & \int d\vec{r}_{q_1 \bar{q}_2} d\vec{r}_{c \bar{c}} d\vec{R}_{\text{total}} d\vec{r}_{q_1 \bar{q}_2, c \bar{c}} \frac{e^{-i\vec{p}'_{q_1 \bar{q}_2} \cdot \vec{r}_{q_1 \bar{q}_2}}}{\sqrt{V}} \frac{e^{-i\vec{p}'_{c \bar{c}} \cdot \vec{r}_{c \bar{c}}}}{\sqrt{V}} \frac{e^{-i\vec{p}'_{q_1 \bar{q}_2, c \bar{c}} \cdot \vec{r}_{q_1 \bar{q}_2, c \bar{c}}}}{\sqrt{V}} \\ & \times \frac{e^{-i\vec{P}_f \cdot \vec{R}_{\text{total}}}}{\sqrt{V}} \varphi_{q_1 \bar{q}_2 c \bar{c} \text{color}}^+ \varphi_{q_1 \bar{q}_2 c \bar{c} \text{flavor}}^+ \varphi_{q_1 \bar{q}_2 c \bar{c} \text{spin}}^+ V_{ab} \psi_A(\vec{r}_{q_1 \bar{q}_2}) \psi_B(\vec{r}_{c \bar{c}}) \\ & \times \frac{e^{i\vec{p}_{AB} \cdot \vec{r}_{AB}}}{\sqrt{V}} \frac{e^{i\vec{P}_i \cdot \vec{R}_{\text{total}}}}{\sqrt{V}} \\ = & (2\pi)^3 \delta^3(\vec{P}_f - \vec{P}_i) \frac{\mathcal{M}_{ab}}{V^3 \sqrt{2E_A 2E_B 2E'_{q_1} 2E'_{\bar{q}_2} 2E'_c 2E'_{\bar{c}}}}, \end{aligned} \quad (4)$$

where \vec{R}_{total} and \vec{P}_f are the center-of-mass coordinate and the total momentum of q_1, \bar{q}_2, c , and \bar{c} , respectively; $\vec{r}_{q_1 \bar{q}_2, c \bar{c}}$ and $\vec{p}'_{q_1 \bar{q}_2, c \bar{c}}$ the relative coordinate and the relative momentum

of the two colored pairs $q_1\bar{q}_2$ and $c\bar{c}$, respectively; $\vec{p}'_{q_1\bar{q}_2}$ the relative momentum of q_1 and \bar{q}_2 , and $\vec{p}'_{c\bar{c}}$ the relative momentum of c and \bar{c} ; \vec{p}_{AB} (\vec{r}_{AB} , \vec{P}_i) the relative momentum (the relative coordinate, the total momentum) of mesons A and B ; E_A , E_B , E'_{q_1} , $E'_{\bar{q}_2}$, E'_c , and $E'_{\bar{c}}$ the energies of A , B , q_1 , \bar{q}_2 , c , and \bar{c} , respectively. \mathcal{M}_{ab} is the transition amplitude corresponding to V_{ab} :

$$\begin{aligned}\mathcal{M}_{ab} = & \sqrt{2E_A 2E_B 2E'_{q_1} 2E'_{\bar{q}_2} 2E'_c 2E'_{\bar{c}}} \\ & \times \int d\vec{r}_{q_1\bar{q}_2} d\vec{r}_{c\bar{c}} d\vec{r}_{q_1\bar{q}_2, c\bar{c}} e^{-i\vec{p}'_{q_1\bar{q}_2} \cdot \vec{r}_{q_1\bar{q}_2} - i\vec{p}'_{c\bar{c}} \cdot \vec{r}_{c\bar{c}} - i\vec{p}'_{q_1\bar{q}_2, c\bar{c}} \cdot \vec{r}_{q_1\bar{q}_2, c\bar{c}}} \\ & \times \varphi_{q_1\bar{q}_2 c\bar{c} \text{color}}^+ \varphi_{q_1\bar{q}_2 c\bar{c} \text{flavor}}^+ \varphi_{q_1\bar{q}_2 c\bar{c} \text{spin}}^+ V_{ab}(\vec{r}_{ab}) \psi_A(\vec{r}_{q_1\bar{q}_2}) \psi_B(\vec{r}_{c\bar{c}}) e^{i\vec{p}_{AB} \cdot \vec{r}_{AB}}.\end{aligned}\quad (5)$$

Let $\phi_{A\text{color}}$ ($\phi_{B\text{color}}$), $\phi_{A\text{flavor}}$ ($\phi_{B\text{flavor}}$), $\phi_{A\text{rel}}$ ($\phi_{B\text{rel}}$), and χ_A (χ_B) stand for the color wave function, the flavor wave function, the quark-antiquark relative-motion wave function, and the spin wave function of meson A (B), respectively; denote the total angular momentum, the orbital angular momentum, and the spin of meson A (B) by J_A (J_B), L_A (L_B), and S_A (S_B), respectively. ψ_A and ψ_B in Eq. (2) are given by

$$\psi_A(\vec{r}_{q_1\bar{q}_2}) = \phi_{A\text{color}} \phi_{A\text{flavor}} (\phi_{A\text{rel}} \chi_A)^{J_A}_{J_{Az}}, \quad (6)$$

$$\psi_B(\vec{r}_{c\bar{c}}) = \phi_{B\text{color}} \phi_{B\text{flavor}} (\phi_{B\text{rel}} \chi_B)^{J_B}_{J_{Bz}}, \quad (7)$$

where J_{Az} (J_{Bz}) is the magnetic projection quantum number of J_A (J_B), and the symbol $(\cdots)^{J_A}_{J_{Az}}$ [$(\cdots)^{J_B}_{J_{Bz}}$] indicates the space-spin wave function of meson A (B). The product of ψ_A and ψ_B is

$$\psi_A(\vec{r}_{q_1\bar{q}_2}) \psi_B(\vec{r}_{c\bar{c}}) = \phi_{A\text{color}} \phi_{B\text{color}} \phi_{A\text{flavor}} \phi_{B\text{flavor}} \sum_{JJ_z} (J_A J_{Az} J_B J_{Bz} | JJ_z) \psi_{\text{in}}^{JJ_z}, \quad (8)$$

where J is the total angular momentum of mesons A and B , and J_z its magnetic projection quantum number; $(J_A J_{Az} J_B J_{Bz} | JJ_z)$ are the Clebsch-Gordan coefficients. Let L (S) and L_z (S_z) denote the total orbital angular momentum (total spin) of mesons A and B and its magnetic projection quantum number, respectively. $\psi_{\text{in}}^{JJ_z}$ comes from the coupling of the space-spin states of meson A and of meson B :

$$\psi_{\text{in}}^{JJ_z} = [(\phi_{A\text{rel}} \chi_A)^{J_A} (\phi_{B\text{rel}} \chi_B)^{J_B}]_{J_z}^J$$

$$\begin{aligned}
&= \sum_{LS} \sqrt{(2J_A + 1)(2J_B + 1)(2L + 1)(2S + 1)} \left\{ \begin{array}{ccc} L_A & S_A & J_A \\ L_B & S_B & J_B \\ L & S & J \end{array} \right\} \\
&\quad \times [(\phi_{A\text{rel}}\phi_{B\text{rel}})^L (\chi_A \chi_B)^S]_{J_z}^J \\
&= \sum_{LSL_zS_z} \sqrt{(2J_A + 1)(2J_B + 1)(2L + 1)(2S + 1)} \left\{ \begin{array}{ccc} L_A & S_A & J_A \\ L_B & S_B & J_B \\ L & S & J \end{array} \right\} \\
&\quad \times (LL_z SS_z |JJ_z) (\phi_{A\text{rel}}\phi_{B\text{rel}})_{L_z}^L (\chi_A \chi_B)_{S_z}^S, \tag{9}
\end{aligned}$$

where the two braces in each of the second and third expressions indicate the Wigner 9j symbol.

Denote by $\phi_{i\text{flavor}}$, ϕ_i , and χ_i the flavor wave function, the space wave function, and the spin wave function of constituent quark or antiquark labeled as i ($i = q_1, \bar{q}_2, c, \bar{c}$), respectively. In fact, ϕ_i equals $e^{i\vec{p}_i' \cdot \vec{r}_i} / \sqrt{V}$ in Eq. (3),

$$\varphi_{q_1 \bar{q}_2 c \bar{c}\text{flavor}} = \phi_{q_1\text{flavor}} \phi_{\bar{q}_2\text{flavor}} c \bar{c}, \tag{10}$$

and

$$\varphi_{q_1 \bar{q}_2 c \bar{c}\text{spin}} = \chi_{q_1} \chi_{\bar{q}_2} \chi_c \chi_{\bar{c}}. \tag{11}$$

The wave function of q_1, \bar{q}_2, c , and \bar{c} is

$$\psi_{q_1 \bar{q}_2 c \bar{c}} = \phi_{q_1} \phi_{\bar{q}_2} \phi_c \phi_{\bar{c}} \varphi_{q_1 \bar{q}_2 c \bar{c}\text{color}} \varphi_{q_1 \bar{q}_2 c \bar{c}\text{flavor}} \varphi_{q_1 \bar{q}_2 c \bar{c}\text{spin}}. \tag{12}$$

After the spin states of q_1 (c) and of \bar{q}_2 (\bar{c}) are coupled to the spin state with the spin $S'_{q_1 + \bar{q}_2}$ ($S'_{c + \bar{c}}$) and its z component $S'_{q_1 + \bar{q}_2 z}$ ($S'_{c + \bar{c} z}$), the spin states with $S'_{q_1 + \bar{q}_2}$ and with $S'_{c + \bar{c}}$ are coupled to the spin state of q_1, \bar{q}_2, c , and \bar{c} , which has the spin S' and its z component S'_z . In this way we have

$$\begin{aligned}
\varphi_{q_1 \bar{q}_2 c \bar{c}\text{spin}} &= \sum_{S'_{q_1 + \bar{q}_2} S'_{q_1 + \bar{q}_2 z}} (s_{q_1} s_{q_1 z} s_{\bar{q}_2} s_{\bar{q}_2 z} | S'_{q_1 + \bar{q}_2} S'_{q_1 + \bar{q}_2 z}) (\chi_{q_1} \chi_{\bar{q}_2})_{S'_{q_1 + \bar{q}_2 z}}^{S'_{q_1 + \bar{q}_2}} \\
&\quad \times \sum_{S'_{c + \bar{c}} S'_{c + \bar{c} z}} (s_c s_{cz} s_{\bar{c}} s_{\bar{c} z} | S'_{c + \bar{c}} S'_{c + \bar{c} z}) (\chi_c \chi_{\bar{c}})_{S'_{c + \bar{c} z}}^{S'_{c + \bar{c}}} \\
&= \sum_{S'_{q_1 + \bar{q}_2} S'_{q_1 + \bar{q}_2 z} S'_{c + \bar{c}} S'_{c + \bar{c} z} S' S'_z} (s_{q_1} s_{q_1 z} s_{\bar{q}_2} s_{\bar{q}_2 z} | S'_{q_1 + \bar{q}_2} S'_{q_1 + \bar{q}_2 z})
\end{aligned}$$

$$\times (s_c s_{cz} s_{\bar{c}} s_{\bar{c}z} | S'_{c+\bar{c}} S'_{c+\bar{c}z}) (S'_{q_1+\bar{q}_2} S'_{q_1+\bar{q}_2 z} S'_{c+\bar{c}} S'_{c+\bar{c}z} | S' S'_z) \psi_{\text{final}}^{S' S'_z}, \quad (13)$$

where s_i is the spin of constituent i , and s_{iz} its z component; the spin wave function $\psi_{\text{final}}^{S' S'_z}$ is

$$\psi_{\text{final}}^{S' S'_z} = [(\chi_{q_1} \chi_{\bar{q}_2})^{S'_{q_1+\bar{q}_2}} (\chi_c \chi_{\bar{c}})^{S'_{c+\bar{c}}}]_{S'_z}. \quad (14)$$

According to Eq. (1), the transition amplitude for $A + B \rightarrow q_1 + \bar{q}_2 + c + \bar{c}$ is

$$\mathcal{M}_{\text{fi}} = \mathcal{M}_{q_1 \bar{c}} + \mathcal{M}_{\bar{q}_2 c} + \mathcal{M}_{q_1 c} + \mathcal{M}_{\bar{q}_2 \bar{c}}, \quad (15)$$

where $\mathcal{M}_{q_1 \bar{c}}$, $\mathcal{M}_{\bar{q}_2 c}$, $\mathcal{M}_{q_1 c}$, and $\mathcal{M}_{\bar{q}_2 \bar{c}}$ correspond to $V_{q_1 \bar{c}}$, $V_{\bar{q}_2 c}$, $V_{q_1 c}$, and $V_{\bar{q}_2 \bar{c}}$, respectively.

Summing over the states of A , B , q_1 , \bar{q}_2 , c , and \bar{c} gives

$$\begin{aligned} \sum_{s_{q_1 z} s_{\bar{q}_2 z} s_{cz} s_{\bar{c}z}} \sum_{J_{Az} J_{Bz}} |\mathcal{M}_{\text{fi}}|^2 &= \sum_{s_{q_1 z} s_{\bar{q}_2 z} s_{cz} s_{\bar{c}z} J_z} |\sqrt{2E_A 2E_B 2E'_{q_1} 2E'_{\bar{q}_2} 2E'_c 2E'_{\bar{c}}} \sum_{ab} \\ &\times \int d\vec{r}_{q_1 \bar{q}_2} d\vec{r}_{cc} d\vec{r}_{q_1 \bar{q}_2, c\bar{c}} e^{-i\vec{p}'_{q_1 \bar{q}_2} \cdot \vec{r}_{q_1 \bar{q}_2} - i\vec{p}'_{cc} \cdot \vec{r}_{cc} - i\vec{p}'_{q_1 \bar{q}_2, c\bar{c}} \cdot \vec{r}_{q_1 \bar{q}_2, c\bar{c}}} \\ &\times \varphi_{q_1 \bar{q}_2 c\bar{c} \text{color}}^+ \varphi_{q_1 \bar{q}_2 c\bar{c} \text{flavor}}^+ \varphi_{q_1 \bar{q}_2 c\bar{c} \text{spin}}^+ V_{ab}(\vec{r}_{ab}) \psi_{\text{in}}^{JJ_z} \\ &\times \phi_{A \text{color}} \phi_{B \text{color}} \phi_{A \text{flavor}} \phi_{B \text{flavor}} e^{i\vec{p}'_{AB} \cdot \vec{r}_{AB}}|^2, \end{aligned} \quad (16)$$

where ab in \sum_{ab} runs through $q_1 \bar{c}$, $\bar{q}_2 c$, $q_1 c$, and $\bar{q}_2 \bar{c}$.

The potential V_{ab} consists of the central spin-independent potential V_{si} and the spin-spin interaction V_{ss} :

$$V_{ab}(\vec{r}_{ab}) = V_{\text{si}}(\vec{r}_{ab}) + V_{\text{ss}}(\vec{r}_{ab}). \quad (17)$$

Below the critical temperature $T_c = 0.175$ GeV, the spin-independent potential is given by

$$V_{\text{si}}(\vec{r}_{ab}) = -\frac{\vec{\lambda}_a}{2} \cdot \frac{\vec{\lambda}_b}{2} \xi_1 \left[1.3 - \left(\frac{T}{T_c} \right)^4 \right] \tanh(\xi_2 r_{ab}) + \frac{\vec{\lambda}_a}{2} \cdot \frac{\vec{\lambda}_b}{2} \frac{6\pi}{25} \frac{v(\lambda r_{ab})}{r_{ab}} \exp(-\xi_3 r_{ab}), \quad (18)$$

where $\xi_1 = 0.525$ GeV, $\xi_2 = 1.5[0.75 + 0.25(T/T_c)^{10}]^6$ GeV, $\xi_3 = 0.6$ GeV, and $\lambda = \sqrt{3b_0/16\pi^2\alpha'}$ in which $\alpha' = 1.04$ GeV $^{-2}$ and $b_0 = 11 - \frac{2}{3}N_f$ with the quark flavor number $N_f = 4$. $\vec{\lambda}_a$ are the Gell-Mann matrices for the color generators of constituent a . The dimensionless function $v(x)$ is given by Buchmüller and Tye [30].

The spin-spin interaction with relativistic effects [31] is [19, 24]

$$V_{ss}(\vec{r}_{ab}) = -\frac{\vec{\lambda}_a}{2} \cdot \frac{\vec{\lambda}_b}{2} \frac{16\pi^2}{25} \frac{d^3}{\pi^{3/2}} \exp(-d^2 r_{ab}^2) \frac{\vec{s}_a \cdot \vec{s}_b}{m_a m_b} + \frac{\vec{\lambda}_a}{2} \cdot \frac{\vec{\lambda}_b}{2} \frac{4\pi}{25} \frac{1}{r_{ab}} \frac{d^2 v(\lambda r_{ab})}{dr_{ab}^2} \frac{\vec{s}_a \cdot \vec{s}_b}{m_a m_b}, \quad (19)$$

where m_a is the mass of constituent a , and d is given by

$$d^2 = d_1^2 \left[\frac{1}{2} + \frac{1}{2} \left(\frac{4m_a m_b}{(m_a + m_b)^2} \right)^4 \right] + d_2^2 \left(\frac{2m_a m_b}{m_a + m_b} \right)^2,$$

where $d_1 = 0.15$ GeV and $d_2 = 0.705$.

One-gluon exchange between constituents a and b gives rise to the Fermi contact term $-\frac{\vec{\lambda}_a}{2} \cdot \frac{\vec{\lambda}_b}{2} \frac{16\pi^2}{25} \delta^3(\vec{r}_{ab}) \frac{\vec{s}_a \cdot \vec{s}_b}{m_a m_b}$ in the nonrelativistic limit. The $\delta^3(\vec{r}_{ab})$ function fixes the positions of the two constituents to $\vec{r}_{ab} = 0$. However, the constituent positions fluctuate because each constituent is coupled to a gluon field which has vacuum polarization. This is similar to the well-known fact that the fluctuation of an electron position arises from vacuum polarization of its coupled electromagnetic field [32, 33]. To take into account this relativistic effect, $\delta^3(\vec{r}_{ab})$ is replaced with $\frac{d^3}{\pi^{3/2}} \exp(-d^2 r_{ab}^2)$ so as to arrive at the first term on the right-hand side of Eq. (19). This is the smearing of the one-gluon-exchange spin-spin interaction [31]. The second term on the right-hand side of Eq. (18) comes from one-gluon exchange plus perturbative one- and two-loop corrections. The second term on the right-hand side of Eq. (19) originates from perturbative one- and two-loop corrections to one-gluon exchange [24]. The loop corrections are another relativistic effect embedded in the spin-independent potential and the spin-spin interaction. Therefore, the potential V_{ab} given in Eq. (17) is a relativized potential.

The potential at short distances is dominated by the the second term of the spin-independent potential and the two terms of the spin-spin interaction. When the center-of-mass energy of mesons A and B is large, short distances are reached by constituents, and the three terms with relativistic effects make a contribution to the scattering of mesons A and B .

The total-spin operator of A and B , i.e., of q_1 , \bar{q}_2 , c , and \bar{c} is

$$\vec{s} = \vec{s}_{q_1} + \vec{s}_{\bar{q}_2} + \vec{s}_c + \vec{s}_{\bar{c}}. \quad (20)$$

It is easily proved that the commutator of \vec{s} and the Hamiltonian that includes V_{ab} equals zero. This leads to $S' = S$ and $S'_z = S_z$. We thus get

$$\begin{aligned}
& \sum_{s_{q_1 z} s_{\bar{q}_2 z} s_{cz} s_{\bar{c}z} J_{Az} J_{Bz}} |\mathcal{M}_{\text{fi}}|^2 \\
&= 2E_A 2E_B 2E'_{q_1} 2E'_{\bar{q}_2} 2E'_c 2E'_{\bar{c}} \\
&\times \sum_{LSJL_z S'_{q_1 + \bar{q}_2} S'_{c + \bar{c}}} (2J_A + 1)(2J_B + 1)(2S + 1)(2J + 1) \left\{ \begin{array}{ccc} L_A & S_A & J_A \\ L_B & S_B & J_B \\ L & S & J \end{array} \right\}^2 \\
&\times \left| \sum_{ab} \int d\vec{r}_{q_1 \bar{q}_2} d\vec{r}_{c\bar{c}} d\vec{r}_{q_1 \bar{q}_2, c\bar{c}} e^{-i\vec{p}'_{q_1 \bar{q}_2} \cdot \vec{r}_{q_1 \bar{q}_2} - i\vec{p}'_{c\bar{c}} \cdot \vec{r}_{c\bar{c}} - i\vec{p}'_{q_1 \bar{q}_2, c\bar{c}} \cdot \vec{r}_{q_1 \bar{q}_2, c\bar{c}} + i\vec{p}_{AB} \cdot \vec{r}_{AB}} \right. \\
&\times \varphi_{q_1 \bar{q}_2 c\bar{c} \text{color}}^+ \varphi_{q_1 \bar{q}_2 c\bar{c} \text{flavor}}^+ \psi_{\text{final}}^{SS_z+} V_{ab}(\vec{r}_{ab}) \phi_{A \text{color}} \phi_{B \text{color}} \phi_{A \text{flavor}} \phi_{B \text{flavor}} (\phi_{A \text{rel}} \phi_{B \text{rel}})_{L_z}^L \\
&\times (\chi_A \chi_B)_{S_z}^S \left. \right|^2. \tag{21}
\end{aligned}$$

We take the Fourier transform of the mesonic quark-antiquark relative-motion wave functions and the potentials:

$$\phi_{A \text{rel}}(\vec{r}_{q_1 \bar{q}_2}) = \int \frac{d^3 p_{q_1 \bar{q}_2}}{(2\pi)^3} \phi_{A \text{rel}}(\vec{p}_{q_1 \bar{q}_2}) e^{i\vec{p}_{q_1 \bar{q}_2} \cdot \vec{r}_{q_1 \bar{q}_2}}, \tag{22}$$

$$\phi_{B \text{rel}}(\vec{r}_{c\bar{c}}) = \int \frac{d^3 p_{c\bar{c}}}{(2\pi)^3} \phi_{B \text{rel}}(\vec{p}_{c\bar{c}}) e^{i\vec{p}_{c\bar{c}} \cdot \vec{r}_{c\bar{c}}}, \tag{23}$$

$$V_{q_1 \bar{c}}(\vec{r}_{q_1 \bar{c}}) = \int \frac{d^3 Q}{(2\pi)^3} V_{q_1 \bar{c}}(\vec{Q}) e^{i\vec{Q} \cdot \vec{r}_{q_1 \bar{c}}}, \tag{24}$$

$$V_{\bar{q}_2 c}(\vec{r}_{\bar{q}_2 c}) = \int \frac{d^3 Q}{(2\pi)^3} V_{\bar{q}_2 c}(\vec{Q}) e^{i\vec{Q} \cdot \vec{r}_{\bar{q}_2 c}}, \tag{25}$$

$$V_{q_1 c}(\vec{r}_{q_1 c}) = \int \frac{d^3 Q}{(2\pi)^3} V_{q_1 c}(\vec{Q}) e^{i\vec{Q} \cdot \vec{r}_{q_1 c}}, \tag{26}$$

$$V_{\bar{q}_2 \bar{c}}(\vec{r}_{\bar{q}_2 \bar{c}}) = \int \frac{d^3 Q}{(2\pi)^3} V_{\bar{q}_2 \bar{c}}(\vec{Q}) e^{i\vec{Q} \cdot \vec{r}_{\bar{q}_2 \bar{c}}}. \tag{27}$$

The quark-antiquark relative-motion wave functions in momentum space, $\phi_{A \text{rel}}(\vec{p}_{q_1 \bar{q}_2})$ and $\phi_{B \text{rel}}(\vec{p}_{c\bar{c}})$, satisfy $\int \frac{d^3 p_{q_1 \bar{q}_2}}{(2\pi)^3} \phi_{A \text{rel}}^+(\vec{p}_{q_1 \bar{q}_2}) \phi_{A \text{rel}}(\vec{p}_{q_1 \bar{q}_2}) = \int \frac{d^3 p_{c\bar{c}}}{(2\pi)^3} \phi_{B \text{rel}}^+(\vec{p}_{c\bar{c}}) \phi_{B \text{rel}}(\vec{p}_{c\bar{c}}) = 1$. We finally arrive at

$$\begin{aligned}
& \sum_{s_{q_1 z} s_{\bar{q}_2 z} s_{cz} s_{\bar{c}z} J_{Az} J_{Bz}} |\mathcal{M}_{\text{fi}}|^2 \\
&= 2E_A 2E_B 2E'_{q_1} 2E'_{\bar{q}_2} 2E'_c 2E'_{\bar{c}}
\end{aligned}$$

$$\begin{aligned}
& \times \sum_{LSJL_z S'_{q_1+\bar{q}_2} S'_{c+\bar{c}}} (2J_A + 1)(2J_B + 1)(2S + 1)(2J + 1) \left\{ \begin{array}{ccc} L_A & S_A & J_A \\ L_B & S_B & J_B \\ L & S & J \end{array} \right\}^2 \\
& \times |\varphi_{q_1 \bar{q}_2 c \bar{c} \text{color}}^+ \varphi_{q_1 \bar{q}_2 c \bar{c} \text{flavor}}^+ \psi_{\text{final}}^{SS_z+} \\
& \times \left\{ V_{q_1 \bar{c}}(\vec{Q}) \left[\phi_{A\text{rel}}(\vec{p}'_{q_1 \bar{q}_2} - \frac{m_{\bar{q}_2}}{m_{q_1} + m_{\bar{q}_2}} \vec{Q}) \phi_{B\text{rel}}(\vec{p}'_{c \bar{c}} - \frac{m_c}{m_c + m_{\bar{c}}} \vec{Q}) \right]_{L_z}^L \right. \\
& + V_{\bar{q}_2 c}(\vec{Q}) \left[\phi_{A\text{rel}}(\vec{p}'_{q_1 \bar{q}_2} + \frac{m_{q_1}}{m_{q_1} + m_{\bar{q}_2}} \vec{Q}) \phi_{B\text{rel}}(\vec{p}'_{c \bar{c}} + \frac{m_{\bar{c}}}{m_c + m_{\bar{c}}} \vec{Q}) \right]_{L_z}^L \\
& + V_{q_1 c}(\vec{Q}) \left[\phi_{A\text{rel}}(\vec{p}'_{q_1 \bar{q}_2} - \frac{m_{\bar{q}_2}}{m_{q_1} + m_{\bar{q}_2}} \vec{Q}) \phi_{B\text{rel}}(\vec{p}'_{c \bar{c}} + \frac{m_{\bar{c}}}{m_c + m_{\bar{c}}} \vec{Q}) \right]_{L_z}^L \\
& \left. + V_{\bar{q}_2 \bar{c}}(\vec{Q}) \left[\phi_{A\text{rel}}(\vec{p}'_{q_1 \bar{q}_2} + \frac{m_{q_1}}{m_{q_1} + m_{\bar{q}_2}} \vec{Q}) \phi_{B\text{rel}}(\vec{p}'_{c \bar{c}} - \frac{m_c}{m_c + m_{\bar{c}}} \vec{Q}) \right]_{L_z}^L \right\} \\
& \times (\chi_A \chi_B)_{S_z}^S |\phi_{A\text{flavor}} \phi_{B\text{flavor}} \phi_{A\text{color}} \phi_{B\text{color}}|^2, \tag{28}
\end{aligned}$$

where \vec{Q} is the gluon momentum.

Let $d\sigma_{\text{free}}$ represent the differential cross section corresponding to the factor $\psi_{\text{final}}^{SS_z+} \sum_{ab} V_{ab} (\phi_{A\text{rel}} \phi_{B\text{rel}})_{L_z}^L (\chi_A \chi_B)_{S_z}^S$ in Eq. (28),

$$\begin{aligned}
d\sigma_{\text{free}} = & \frac{(2\pi)^4}{4\sqrt{(P_A \cdot P_B)^2 - m_A^2 m_B^2}} \frac{d^3 p'_{q_1}}{(2\pi)^3 2E'_{q_1}} \frac{d^3 p'_{\bar{q}_2}}{(2\pi)^3 2E'_{\bar{q}_2}} \frac{d^3 p'_{c}}{(2\pi)^3 2E'_{c}} \frac{d^3 p'_{\bar{c}}}{(2\pi)^3 2E'_{\bar{c}}} \\
& \times \delta^4(P_A + P_B - p'_{q_1} - p'_{\bar{q}_2} - p'_{c} - p'_{\bar{c}}) \\
& \times 2E_A 2E_B 2E'_{q_1} 2E'_{\bar{q}_2} 2E'_{c} |\varphi_{q_1 \bar{q}_2 c \bar{c} \text{color}}^+ \varphi_{q_1 \bar{q}_2 c \bar{c} \text{flavor}}^+ \psi_{\text{final}}^{SS_z+} \\
& \times \left\{ V_{q_1 \bar{c}}(\vec{Q}) \left[\phi_{A\text{rel}}(\vec{p}'_{q_1 \bar{q}_2} - \frac{m_{\bar{q}_2}}{m_{q_1} + m_{\bar{q}_2}} \vec{Q}) \phi_{B\text{rel}}(\vec{p}'_{c \bar{c}} - \frac{m_c}{m_c + m_{\bar{c}}} \vec{Q}) \right]_{L_z}^L \right. \\
& + V_{\bar{q}_2 c}(\vec{Q}) \left[\phi_{A\text{rel}}(\vec{p}'_{q_1 \bar{q}_2} + \frac{m_{q_1}}{m_{q_1} + m_{\bar{q}_2}} \vec{Q}) \phi_{B\text{rel}}(\vec{p}'_{c \bar{c}} + \frac{m_{\bar{c}}}{m_c + m_{\bar{c}}} \vec{Q}) \right]_{L_z}^L \\
& + V_{q_1 c}(\vec{Q}) \left[\phi_{A\text{rel}}(\vec{p}'_{q_1 \bar{q}_2} - \frac{m_{\bar{q}_2}}{m_{q_1} + m_{\bar{q}_2}} \vec{Q}) \phi_{B\text{rel}}(\vec{p}'_{c \bar{c}} + \frac{m_{\bar{c}}}{m_c + m_{\bar{c}}} \vec{Q}) \right]_{L_z}^L \\
& \left. + V_{\bar{q}_2 \bar{c}}(\vec{Q}) \left[\phi_{A\text{rel}}(\vec{p}'_{q_1 \bar{q}_2} + \frac{m_{q_1}}{m_{q_1} + m_{\bar{q}_2}} \vec{Q}) \phi_{B\text{rel}}(\vec{p}'_{c \bar{c}} - \frac{m_c}{m_c + m_{\bar{c}}} \vec{Q}) \right]_{L_z}^L \right\} \\
& \times (\chi_A \chi_B)_{S_z}^S |\phi_{A\text{flavor}} \phi_{B\text{flavor}} \phi_{A\text{color}} \phi_{B\text{color}}|^2, \tag{29}
\end{aligned}$$

where m_A (m_B) is the mass of meson A (B); $P_A = (E_A, \vec{P}_A)$, $P_B = (E_B, \vec{P}_B)$, $s = (P_A + P_B)^2$, and $p'_i = (E'_i, \vec{p}'_i)$ with $i = q_1, \bar{q}_2, c$, and \bar{c} . $d\sigma_{\text{free}}$ depends on L_A, S_A, L_B, S_B, L, S ,

L_z , $S'_{q_1+\bar{q}_2}$, and $S'_{c+\bar{c}}$. The unpolarized differential cross section for $A+B \rightarrow q_1+\bar{q}_2+c+\bar{c}$ is thus

$$\begin{aligned} d\sigma_{\text{free}}^{\text{unpol}}(\sqrt{s}, T) &= \frac{(2\pi)^4}{4\sqrt{(P_A \cdot P_B)^2 - m_A^2 m_B^2}} \frac{d^3 p'_{q_1}}{(2\pi)^3 2E'_{q_1}} \frac{d^3 p'_{\bar{q}_2}}{(2\pi)^3 2E'_{\bar{q}_2}} \frac{d^3 p'_{c}}{(2\pi)^3 2E'_{c}} \frac{d^3 p'_{\bar{c}}}{(2\pi)^3 2E'_{\bar{c}}} \\ &\times \delta^4(P_A + P_B - p'_{q_1} - p'_{\bar{q}_2} - p'_{c} - p'_{\bar{c}}) \sum_{s_{q_1 z} s_{\bar{q}_2 z} s_{c z} s_{\bar{c} z} J_{A z} J_{B z}} |\mathcal{M}_{\text{fi}}|^2 \\ &= \sum_{LSJL_z S'_{q_1+\bar{q}_2} S'_{c+\bar{c}}} (2S+1)(2J+1) \left\{ \begin{array}{ccc} L_A & S_A & J_A \\ L_B & S_B & J_B \\ L & S & J \end{array} \right\}^2 d\sigma_{\text{free}}. \quad (30) \end{aligned}$$

Now we give the cross section for $A+B \rightarrow q_1+\bar{q}_2+c+\bar{c} \rightarrow H_c + X$, which includes the fragmentation process $c \rightarrow H_c$. Denote by z the fraction of energy passed on from quark c to hadron H_c . The fragmentation function $D_c^{H_c}(z, \mu^2)$ at the factorization scale μ indicates that $D_c^{H_c}(z, \mu^2)dz$ is the number of hadron H_c produced at z and within dz . Consequently, the unpolarized differential cross section for $A+B \rightarrow q_1+\bar{q}_2+c+\bar{c} \rightarrow H_c + X$ is

$$\begin{aligned} d\sigma^{\text{unpol}}(\sqrt{s}, T) &= d\sigma_{\text{free}}^{\text{unpol}}(\sqrt{s}, T) D_c^{H_c}(z, \mu^2) dz \\ &= \sum_{LSJL_z S'_{q_1+\bar{q}_2} S'_{c+\bar{c}}} (2S+1)(2J+1) \left\{ \begin{array}{ccc} L_A & S_A & J_A \\ L_B & S_B & J_B \\ L & S & J \end{array} \right\}^2 d\sigma_{\text{free}} D_c^{H_c}(z, \mu^2) dz. \quad (31) \end{aligned}$$

The present work involves the three cases: $L_A = 0, L_B = 0$; $L_A = 0, L_B \neq 0, S_A = 0$; $L_A = 0, L_B = 1, S_A = 1, S_B = 1$. Values of the Wigner $9j$ symbol in these cases reduce the unpolarized differential cross section to

$$d\sigma^{\text{unpol}}(\sqrt{s}, T) = \frac{1}{(2S_A+1)(2S_B+1)(2L_B+1)} \sum_{L_B z S S'_{q_1+\bar{q}_2} S'_{c+\bar{c}}} (2S+1) d\sigma_{\text{free}} D_c^{H_c}(z, \mu^2) dz. \quad (32)$$

The unpolarized cross section for $A+B \rightarrow q_1+\bar{q}_2+c+\bar{c} \rightarrow H_c + X$ is

$$\sigma^{\text{unpol}}(\sqrt{s}, T) = \frac{1}{(2S_A+1)(2S_B+1)(2L_B+1)} \sum_{L_B z S S'_{q_1+\bar{q}_2} S'_{c+\bar{c}}} (2S+1) \sigma(\sqrt{s}, T), \quad (33)$$

with

$$\sigma(\sqrt{s}, T) = \int d\sigma_{\text{free}} D_c^{H_c}(z, \mu^2) dz. \quad (34)$$

The cross section depends on temperature and the center-of-mass energy \sqrt{s} of mesons A and B .

3. Numerical results and discussions

For large-momentum charmonia we consider the following charmonium dissociation reactions:

$$\pi + J/\psi \rightarrow H_c + X, \pi + \psi' \rightarrow H_c + X, \pi + \chi_c \rightarrow H_c + X,$$

$$\rho + J/\psi \rightarrow H_c + X, \rho + \psi' \rightarrow H_c + X, \rho + \chi_c \rightarrow H_c + X,$$

$$K + J/\psi \rightarrow H_c + X, K + \psi' \rightarrow H_c + X, K + \chi_c \rightarrow H_c + X,$$

$$K^* + J/\psi \rightarrow H_c + X, K^* + \psi' \rightarrow H_c + X, K^* + \chi_c \rightarrow H_c + X,$$

where H_c is D^+ , D^0 , D_s^+ , or D^{*+} . We solve the Schrödinger equation with the potential given in Eq. (17) to obtain $\phi_{A\text{rel}}(\vec{r}_{q_1\bar{q}_2})$, $\phi_{B\text{rel}}(\vec{r}_{c\bar{c}})$, and temperature-dependent meson masses where the up-quark mass, the strange-quark mass, and the charm-quark mass are 0.32, 0.5, and 1.51 GeV, respectively. The momentum-space wave functions [$\phi_{A\text{rel}}(\vec{p}_{q_1\bar{q}_2})$ and $\phi_{B\text{rel}}(\vec{p}_{c\bar{c}})$] appearing in Eqs. (22) and (23) are used in Eq. (29) to calculate $d\sigma_{\text{free}}$.

According to Eqs. (17)-(19) and (29), we need to calculate the color matrix elements $\varphi_{q_1\bar{q}_2 c\bar{c}\text{color}}^+ \frac{\vec{\lambda}_a}{2} \cdot \frac{\vec{\lambda}_b}{2} \phi_{A\text{color}} \phi_{B\text{color}}$. $\varphi_{q_1\bar{q}_2 c\bar{c}\text{color}}$ is derived in the appendix. Corresponding to the potentials $V_{q_1\bar{c}}$, $V_{\bar{q}_2 c}$, $V_{q_1 c}$, and $V_{\bar{q}_2 \bar{c}}$, the color matrix elements are

$$\varphi_{q_1\bar{q}_2 c\bar{c}\text{color}}^+ \frac{\vec{\lambda}_{q_1}}{2} \cdot \frac{\vec{\lambda}_{\bar{c}}}{2} \phi_{A\text{color}} \phi_{B\text{color}} = -\frac{\sqrt{6}}{9}, \quad (35)$$

$$\varphi_{q_1\bar{q}_2 c\bar{c}\text{color}}^+ \frac{\vec{\lambda}_{\bar{q}_2}}{2} \cdot \frac{\vec{\lambda}_c}{2} \phi_{A\text{color}} \phi_{B\text{color}} = -\frac{\sqrt{6}}{9}, \quad (36)$$

$$\varphi_{q_1\bar{q}_2 c\bar{c}\text{color}}^+ \frac{\vec{\lambda}_{q_1}}{2} \cdot \frac{\vec{\lambda}_c}{2} \phi_{A\text{color}} \phi_{B\text{color}} = \frac{\sqrt{6}}{9}, \quad (37)$$

$$\varphi_{q_1\bar{q}_2 c\bar{c}\text{color}}^+ \frac{\vec{\lambda}_{\bar{q}_2}}{2} \cdot \frac{\vec{\lambda}_{\bar{c}}}{2} \phi_{A\text{color}} \phi_{B\text{color}} = \frac{\sqrt{6}}{9}. \quad (38)$$

The flavor matrix elements $\varphi_{q_1\bar{q}_2 c\bar{c}\text{flavor}}^+ \phi_{A\text{flavor}} \phi_{B\text{flavor}}$ in Eq. (29) are 1.

According to Eqs. (17)-(19) and (29), we calculate $\psi_{\text{final}}^{SS_z+}(\chi_A \chi_B)_{S_z}^S$ for the central spin-independent potential and $\psi_{\text{final}}^{SS_z+} \vec{s}_a \cdot \vec{s}_b (\chi_A \chi_B)_{S_z}^S$ for the spin-spin interaction. These spin matrix elements are listed in Table 1. They are independent of S_z , and $d\sigma_{\text{free}}$ is thus independent of S_z .

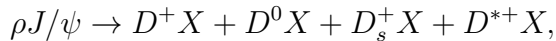
The charm-quark fragmentation functions used in Eq. (34) are solutions of the Dokshitzer-Gribov-Lipatov-Altarelli-Paris (DGLAP) evolution equations with $\mu = \sqrt{s}$ [34, 35]. The starting point for the DGLAP evolution in μ is taken to be the charm-quark mass. Unpolarized cross sections for charmonium dissociation in collisions with π , ρ , K , and K^* mesons are calculated with Eq. (33). For the convenient use of the unpolarized cross sections, they are parametrized as

$$\begin{aligned} \sigma^{\text{unpol}}(\sqrt{s}, T) = & a_1 \left(\frac{\sqrt{s} - \sqrt{s_0}}{b_1} \right)^{c_1} \exp \left[c_1 \left(1 - \frac{\sqrt{s} - \sqrt{s_0}}{b_1} \right) \right] \\ & + a_2 \left(\frac{\sqrt{s} - \sqrt{s_0}}{b_2} \right)^{c_2} \exp \left[c_2 \left(1 - \frac{\sqrt{s} - \sqrt{s_0}}{b_2} \right) \right], \end{aligned} \quad (39)$$

where $\sqrt{s_0}$ is the threshold energy and equals the sum of the H_c mass, the \bar{D} mass, the q_1 mass, and the \bar{q}_2 mass. The values of the parameters, a_1 , b_1 , c_1 , a_2 , b_2 , and c_2 , are listed in Tables 2-10. In these tables, d_0 is the separation between the peak's location on the \sqrt{s} -axis and the threshold energy, and $\sqrt{s_z}$ is the square root of the Mandelstam variable at which the cross section is 1/100 of the peak cross section that is obtained from the parametrization. We note that the parametrization of a reaction at a given temperature is valid in the \sqrt{s} region where the cross-section curve for the reaction is displayed below.

Cross sections for the pion-charmonium reactions were obtained with an early version of FORTRAN code in Ref. [28]. After an error is removed, a new version is used to calculate pion-charmonium dissociation cross sections, which are smaller than those shown in Ref. [28]. We do not plot the cross sections, but list values of a_1 , b_1 , c_1 , a_2 , b_2 , c_2 , d_0 , and $\sqrt{s_z}$ in Tables 11-13.

In Figs. 1-9 we plot unpolarized cross sections for the following reactions:



$$\rho\chi_c \rightarrow D^+X + D^0X + D_s^+X + D^{*+}X,$$

$$KJ/\psi \rightarrow D^+X + D^0X + D_s^+X + D^{*+}X,$$

$$K\psi' \rightarrow D^+X + D^0X + D_s^+X + D^{*+}X,$$

$$K\chi_c \rightarrow D^+X + D^0X + D_s^+X + D^{*+}X,$$

$$K^*J/\psi \rightarrow D^+X + D^0X + D_s^+X + D^{*+}X,$$

$$K^*\psi' \rightarrow D^+X + D^0X + D_s^+X + D^{*+}X,$$

$$K^*\chi_c \rightarrow D^+X + D^0X + D_s^+X + D^{*+}X.$$

Since mesons A and B are broken up in the reaction $A + B \rightarrow q_1 + \bar{q}_2 + c + \bar{c}$, the produced constituents q_1 , \bar{q}_2 , c , and \bar{c} are described by plane waves. The first term on the right-hand side of Eq. (18) stands for the confining potential. In the confinement regime the mesonic quark-antiquark relative-motion wave functions are mainly determined by the confining potential, and are nonperturbative. The perturbative part of the mesonic quark-antiquark relative-motion wave functions is mainly determined by the second term on the right-hand side of Eq. (18) and the spin-spin interaction. At low energies near threshold, the nonperturbative part of the wave functions of mesons A and B overlap, and it is very difficult for the collision of mesons A and B to break them to produce plane waves of q_1 , \bar{q}_2 , c , and \bar{c} . Therefore, the unpolarized cross sections near threshold are negligible. With increasing \sqrt{s} , more and more the perturbative part of the meson wave functions is probed, the production of plane waves gradually increases, and the cross sections increase.

We present the unpolarized cross sections in the \sqrt{s} region that are generally accessed by collisions between light mesons in hadronic matter and the three charmonia (J/ψ , ψ' , and χ_c). Cross sections for some reactions at some temperatures reach maximum values around $\sqrt{s} = 11$ GeV. Examples are the cross sections for $\rho J/\psi \rightarrow D^{*+}X$ at $T/T_c = 0.95$ in Fig. 10, $\rho\psi' \rightarrow D_s^+X$ at $T/T_c = 0.65, 0.75, 0.85, 0.9$, and 0.95 in Fig. 11, and $K^*\chi_c \rightarrow D^0X$ at $T/T_c = 0.85$ and 0.9 in Fig. 12. Therefore, we use $\sqrt{s} = 11$ GeV in discussions in the next two paragraphs.

At large \sqrt{s} values, the dependence of the cross sections on temperature is obvious. For example, at $\sqrt{s} = 11$ GeV the cross sections for $\rho J/\psi$ reactions decrease with increasing temperature, but the cross sections for $\rho\psi'$, $\rho\chi_c$, K +charmonium, and K^* +charmonium reactions increase first and then decrease. Denote by $\sigma_{11\min}$ ($\sigma_{11\max}$) the smallest (largest) cross section among the six cross sections corresponding to $T/T_c=0, 0.65, 0.75, 0.85, 0.9$, and 0.95 at $\sqrt{s}=11$ GeV. Since $\sigma_{11\min}$ is the cross section at $T/T_c=0.95$ as seen in Figs. 1-9, it is used as a benchmark to see the temperature dependence of cross sections for all reactions. The ratio of $\sigma_{11\max}$ to $\sigma_{11\min}$ may represent the variation of the cross section with respect to temperature. For example, from the dashed curve and the dot-dot-dashed curve in Fig. 8, $\sigma_{11\max}/\sigma_{11\min}$ equals 7.46 for $K^*\psi' \rightarrow D^+X + D^0X + D_s^+X + D^{*+}X$. The value indicates that the cross sections for $K^*\psi'$ reactions change rapidly with increasing temperature. In order of decrease of $\sigma_{11\max}/\sigma_{11\min}$, we list the reactions that produce D^+X , D^0X , D_s^+X , and $D^{*+}X$: $K^*\psi'$, $\rho\psi'$, $K^*\chi_c$, $\rho\chi_c$, $K\psi'$, K^*J/ψ , $\rho J/\psi$, $\pi\psi'$, $K\chi_c$, $\pi\chi_c$, KJ/ψ , and $\pi J/\psi$.

A low-energy reaction between a light meson and a charmonium produces two charmed mesons. While \sqrt{s} increases from threshold, the cross section for every endothermic reaction rises from zero, arrives at a maximum value, and decreases, but the cross section for every exothermic reaction decreases rapidly from infinity and then may increase, reaching a maximum and decreasing. Peak cross sections of J/ψ dissociation in collisions with π , ρ , K , and K^* mesons are collected from some references, and are listed in Table 14. In the last row of the table, we show cross sections at $\sqrt{s} = 11$ GeV and $T = 0$ GeV for $\pi J/\psi \rightarrow D^+X + D^0X + D_s^+X + D^{*+}X + D^{*0}X + D_s^{*+}X$, $\rho J/\psi \rightarrow D^+X + D^0X + D_s^+X + D^{*+}X + D_s^{*0}X + D_s^{*+}X$, $KJ/\psi \rightarrow D^+X + D^0X + D_s^+X + D^{*+}X + D^{*0}X + D_s^{*+}X$, and $K^*J/\psi \rightarrow D^+X + D^0X + D_s^+X + D^{*+}X + D^{*0}X + D_s^{*+}X$, which are obtained in the present work. Since $c \rightarrow D^{*0}$ and $c \rightarrow D_s^{*+}$ fragmentation functions are unknown, cross sections for $\pi J/\psi \rightarrow D^{*0}X$, $\pi J/\psi \rightarrow D_s^{*+}X$, $\rho J/\psi \rightarrow D^{*0}X$, $\rho J/\psi \rightarrow D_s^{*+}X$, $KJ/\psi \rightarrow D^{*0}X$, $KJ/\psi \rightarrow D_s^{*+}X$, $K^*J/\psi \rightarrow D^{*0}X$, and $K^*J/\psi \rightarrow D_s^{*+}X$ are not calculated. In order to estimate the eight cross sections at $\sqrt{s} = 11$ GeV and $T = 0$ GeV, it is assumed that the ratio of the cross section for inclusive D^{*0} (D_s^{*+}) production to the one for inclusive D^{*+}

production equals the ratio of the one for inclusive D^0 (D_s^+) production to the one for inclusive D^+ production, that is,

$$\frac{\sigma_{\pi J/\psi \rightarrow D^{*0}X}^{\text{unpol}}}{\sigma_{\pi J/\psi \rightarrow D^{*+}X}^{\text{unpol}}} = \frac{\sigma_{\pi J/\psi \rightarrow D^0X}^{\text{unpol}}}{\sigma_{\pi J/\psi \rightarrow D^+X}^{\text{unpol}}},$$

$$\frac{\sigma_{\pi J/\psi \rightarrow D_s^{*+}X}^{\text{unpol}}}{\sigma_{\pi J/\psi \rightarrow D^{*+}X}^{\text{unpol}}} = \frac{\sigma_{\pi J/\psi \rightarrow D_s^+X}^{\text{unpol}}}{\sigma_{\pi J/\psi \rightarrow D^+X}^{\text{unpol}}},$$

$$\frac{\sigma_{\rho J/\psi \rightarrow D^{*0}X}^{\text{unpol}}}{\sigma_{\rho J/\psi \rightarrow D^{*+}X}^{\text{unpol}}} = \frac{\sigma_{\rho J/\psi \rightarrow D^0X}^{\text{unpol}}}{\sigma_{\rho J/\psi \rightarrow D^+X}^{\text{unpol}}},$$

and so on. It is shown from the table that the cross sections at high \sqrt{s} in the present work are comparable to those peak cross sections at low \sqrt{s} .

4. Summary

We have obtained temperature-dependent cross sections for dissociation of large-momentum charmonia in collisions with π , ρ , K , and K^* mesons in a mechanism where the collision between a light meson and a charmonium produces two quarks and two antiquarks first, then the charm quark fragments into charmed mesons, and the other three constituents combine with quarks and antiquarks created from vacuum to form two or more mesons. According to the mechanism, we have derived the transition amplitude for $A + B \rightarrow q_1 + \bar{q}_2 + c + \bar{c}$ from the wave functions of mesons A and B and of q_1 , \bar{q}_2 , c , and \bar{c} . An expression for the absolute square of the transition amplitude is derived from the mesonic quark-antiquark relative-motion wave functions and the spin wave functions. The color wave function of q_1 , \bar{q}_2 , c , and \bar{c} is derived in group representation theory. With the charm-quark fragmentation functions, the unpolarized cross section for $A + B \rightarrow q_1 + \bar{q}_2 + c + \bar{c} \rightarrow H_c + X$ is derived. We have calculated the color, flavor, and spin matrix elements. The mesonic quark-antiquark relative-motion wave functions result from the Schrödinger equation with the temperature-dependent quark potential. We have provided parametrizations of the numerical unpolarized cross sections.

The unpolarized cross sections for inclusive D^+ , D^0 , D_s^+ , and D^{*+} production increase with increasing center-of-mass energy of the colliding light meson and charmonium, de-

pending on the contributions of the nonperturbative part and the perturbative part of the quark-antiquark relative-motion wave functions of the colliding mesons. At high \sqrt{s} the change of the unpolarized cross sections with increasing temperature is obvious. Compared to the peak cross sections obtained in the effective meson approach and in the quark-interchange approach at low \sqrt{s} , a similar scale of cross sections at high \sqrt{s} has been obtained.

Acknowledgements

This work was supported by the National Natural Science Foundation of China under Grant No. 11175111.

Appendix: The color wave function of q_1 , \bar{q}_2 , c , and \bar{c}

Based on Ref. [36], we provide a way to construct the color wave function of q_1 , \bar{q}_2 , c , and \bar{c} that are produced in a collision of mesons A and B . The three color wave functions of a quark (an antiquark) are denoted by r , g , and b (\bar{r} , \bar{g} , and \bar{b}), respectively. To apply a permutation group to obtain the color wave function $\varphi_{q_1\bar{q}_2cc\text{color}}$, we use 1, 2, 3, and 4 to label q_1 , \bar{q}_2 , c , and \bar{c} , respectively. The numbers 1 and 2 form a S_2 group, and the numbers 3 and 4 form another S_2 group. The direct product of the two permutation groups is the group that has the following four elements:

$$R_1 = \begin{pmatrix} 1 & 2 & 3 & 4 \\ 1 & 2 & 3 & 4 \end{pmatrix}, \quad R_2 = \begin{pmatrix} 1 & 2 & 3 & 4 \\ 2 & 1 & 3 & 4 \end{pmatrix}, \quad R_3 = \begin{pmatrix} 1 & 2 & 3 & 4 \\ 1 & 2 & 4 & 3 \end{pmatrix}, \quad R_4 = \begin{pmatrix} 1 & 2 & 3 & 4 \\ 2 & 1 & 4 & 3 \end{pmatrix}.$$

Each group element forms a class, and the $S_2 \times S_2$ group has four classes. The class operator is defined as the sum of all group elements in the class. The group has the following four class operators:

$$C_1 = R_1, \quad C_2 = R_2, \quad C_3 = R_3, \quad C_4 = R_4. \quad (40)$$

In the class space, the class operators give

$$C_i C_j = \sum_{k=1}^4 D_{kj}(C_i) C_k, \quad (41)$$

where $D_{kj}(C_i)$ form a matrix that defines a representation of C_i as

$$D(C_1) = \begin{pmatrix} 1 & 0 & 0 & 0 \\ 0 & 1 & 0 & 0 \\ 0 & 0 & 1 & 0 \\ 0 & 0 & 0 & 1 \end{pmatrix}, \quad D(C_2) = \begin{pmatrix} 0 & 1 & 0 & 0 \\ 1 & 0 & 0 & 0 \\ 0 & 0 & 0 & 1 \\ 0 & 0 & 1 & 0 \end{pmatrix},$$

$$D(C_3) = \begin{pmatrix} 0 & 0 & 1 & 0 \\ 0 & 0 & 0 & 1 \\ 1 & 0 & 0 & 0 \\ 0 & 1 & 0 & 0 \end{pmatrix}, \quad D(C_4) = \begin{pmatrix} 0 & 0 & 0 & 1 \\ 0 & 0 & 1 & 0 \\ 0 & 1 & 0 & 0 \\ 1 & 0 & 0 & 0 \end{pmatrix}.$$

Let Q and λ_i individually stand for the eigenvector and the eigenvalue of C_i in the class space, and Q is expressed as

$$Q = \sum_{j=1}^4 q_j C_j, \quad (42)$$

where q_j are determined by

$$C_i Q = \lambda_i Q, \quad (43)$$

that is,

$$\left[D(C_i) - \lambda_i \begin{pmatrix} 1 & 0 & 0 & 0 \\ 0 & 1 & 0 & 0 \\ 0 & 0 & 1 & 0 \\ 0 & 0 & 0 & 1 \end{pmatrix} \right] \begin{pmatrix} q_1 \\ q_2 \\ q_3 \\ q_4 \end{pmatrix} = 0. \quad (44)$$

Solving the above equations, we get the projection operator which differs from Q by a constant:

$$P = q_4(C_1 + C_2 + C_3 + C_4). \quad (45)$$

Let P operate on the following six color wave functions:

$$\varphi_1 = r(1)r(2)\bar{r}(3)\bar{r}(4), \quad (46)$$

$$\varphi_2 = g(1)g(2)\bar{g}(3)\bar{g}(4), \quad (47)$$

$$\varphi_3 = b(1)b(2)\bar{b}(3)\bar{b}(4), \quad (48)$$

$$\varphi_4 = r(1)g(2)\bar{r}(3)\bar{g}(4), \quad (49)$$

$$\varphi_5 = g(1)b(2)\bar{g}(3)\bar{b}(4), \quad (50)$$

$$\varphi_6 = b(1)r(2)\bar{b}(3)\bar{r}(4), \quad (51)$$

and then add normalized $P\varphi_1$, $P\varphi_2$, $P\varphi_3$, $P\varphi_4$, $P\varphi_5$, and $P\varphi_6$ to give the color singlet of q_1 , \bar{q}_2 , c , and \bar{c} ,

$$\begin{aligned} \varphi_{q_1\bar{q}_2c\bar{c}\text{color}} = & \frac{1}{\sqrt{6}} \left\{ r(1)r(2)\bar{r}(3)\bar{r}(4) + g(1)g(2)\bar{g}(3)\bar{g}(4) + b(1)b(2)\bar{b}(3)\bar{b}(4) \right. \\ & + \frac{1}{2}[r(1)g(2)\bar{r}(3)\bar{g}(4) + r(2)g(1)\bar{r}(3)\bar{g}(4) + r(1)g(2)\bar{r}(4)\bar{g}(3) \\ & + r(2)g(1)\bar{r}(4)\bar{g}(3)] + \frac{1}{2}[g(1)b(2)\bar{g}(3)\bar{b}(4) + g(2)b(1)\bar{g}(3)\bar{b}(4) \\ & + g(1)b(2)\bar{g}(4)\bar{b}(3) + g(2)b(1)\bar{g}(4)\bar{b}(3)] + \frac{1}{2}[b(1)r(2)\bar{b}(3)\bar{r}(4) \\ & \left. + b(2)r(1)\bar{b}(3)\bar{r}(4) + b(1)r(2)\bar{b}(4)\bar{r}(3) + b(2)r(1)\bar{b}(4)\bar{r}(3)] \right\}. \end{aligned} \quad (52)$$

It satisfies

$$(\vec{\lambda}_{q_1} + \vec{\lambda}_{\bar{q}_2} + \vec{\lambda}_c + \vec{\lambda}_{\bar{c}})\varphi_{q_1\bar{q}_2c\bar{c}\text{color}} = 0. \quad (53)$$

Denote by ϕ_{q_1cm} ($\phi_{\bar{q}_2cm}$, ϕ_{ccm} , $\phi_{\bar{c}cm}$) the color wave function of q_1 (\bar{q}_2 , c , \bar{c}). When m runs from 1 to 3, ϕ_{q_1cm} and ϕ_{ccm} are r , g , and b , and $\phi_{\bar{q}_2cm}$ and $\phi_{\bar{c}cm}$ are \bar{r} , \bar{g} , and \bar{b} , respectively. With this notation the color singlet is given by the short expression,

$$\varphi_{q_1\bar{q}_2c\bar{c}\text{color}} = \frac{1}{2\sqrt{6}} \sum_{m=1}^3 \sum_{n=1}^3 (\phi_{q_1cm}\phi_{ccn}\phi_{\bar{q}_2cm}\phi_{\bar{c}cn} + \phi_{q_1cm}\phi_{ccn}\phi_{\bar{q}_2cn}\phi_{\bar{c}cm}). \quad (54)$$

References

- [1] D. Kharzeev and H. Satz, Phys. Lett. B 334, 155 (1994).
- [2] M. E. Peskin, Nucl. Phys. B 156, 365 (1979); G. Bhanot and M. E. Peskin, Nucl. Phys. B 156, 391 (1979).
- [3] F. Arleo, P. B. Gossiaux, T. Gousset, and J. Aichelin, Phys. Rev. D 65, 014005 (2001).
- [4] S. G. Matinyan and B. Müller, Phys. Rev. C 58, 2994 (1998).

- [5] K. L. Haglin, Phys. Rev. C 61, 031902(R) (2000); K. L. Haglin and C. Gale, Phys. Rev. C 63, 065201 (2001).
- [6] Z. Lin and C. M. Ko, Phys. Rev. C 62, 034903 (2000); J. Phys. G 27, 617 (2001).
- [7] Y. S. Oh, T. S. Song, and S. H. Lee, Phys. Rev. C 63, 034901 (2001).
- [8] F. S. Navarra, M. Nielsen, and M. R. Robilotta, Phys. Rev. C 64, 021901(R) (2001).
- [9] L. Maiani, F. Piccinini, A. D. Polosa, and V. Riquer, Nucl. Phys. A 741, 273 (2004).
- [10] R. S. Azevedo and M. Nielsen, Phys. Rev. C 69, 035201 (2004).
- [11] A. Bourque and C. Gale, Phys. Rev. C 80, 015204 (2009).
- [12] M. Cleven, V. K. Magas, and A. Ramos, Phys. Rev. C 96, 045201 (2017).
- [13] L. M. Abreu, K. P. Khemchandani, A. M. Torres, F. S. Navarra, and M. Nielsen, Phys. Rev. C 97, 044902 (2018).
- [14] L. M. Abreu, E. Cavalcanti, and A. P. C. Malbouisson, Nucl. Phys. A 978, 107 (2018).
- [15] T. Barnes and E. S. Swanson, Phys. Rev. D 46, 131 (1992); E. S. Swanson, Ann. Phys. (N.Y.) 220, 73 (1992).
- [16] K. Martins, D. Blaschke, and E. Quack, Phys. Rev. C 51, 2723 (1995).
- [17] C.-Y. Wong, E. S. Swanson, and T. Barnes, Phys. Rev. C 62, 045201 (2000); Phys. Rev. C 65, 014903 (2001).
- [18] T. Barnes, E. S. Swanson, C.-Y. Wong, and X.-M. Xu, Phys. Rev. C 68, 014903 (2003).
- [19] J. Zhou and X.-M. Xu, Phys. Rev. C 85, 064904 (2012).
- [20] S.-T. Ji, Z.-Y. Shen, and X.-M. Xu, J. Phys. G 42, 095110 (2015).
- [21] F.-R. Liu, S.-T. Ji, and X.-M. Xu, J. Korean Phys. Soc. 69, 472 (2016).

- [22] F. O. Durães, H. Kim, S. H. Lee, F. S. Navarra, and M. Nielsen, Phys. Rev. C 68, 035208 (2003).
- [23] C.-Y. Wong, Phys. Rev. C 65, 034902 (2002).
- [24] X.-M. Xu, Nucl. Phys. A 697, 825 (2002).
- [25] L. M. Abreu and H. P. L. Vieira, Eur. Phys. J. A 57, 163 (2021).
- [26] A. M. Sirunyan *et al.*, Eur. Phys. J. C 78, 509 (2018).
- [27] M. Aaboud *et al.*, Eur. Phys. J. C 78, 762 (2018).
- [28] S.-T. Ji, X.-M. Xu, and H. J. Weber, Nucl. Phys. A 966, 224 (2017).
- [29] R. D. Field and R. P. Feynman, Nucl. Phys. B 136, 1 (1978); R. D. Field, *Applications of Perturbative QCD* (Addison-Wesley, Redwood City, CA, 1989).
- [30] W. Buchmüller and S.-H. H. Tye, Phys. Rev. D 24, 132 (1981).
- [31] S. Godfrey and N. Isgur, Phys. Rev. D 32, 189 (1985).
- [32] J. D. Bjorken and S. D. Drell, *Relativistic Quantum Mechanics* (McGraw-Hill, New York, 1964).
- [33] F. Schwabl, *Quantum Mechanics* (Springer-Verlag, Berlin, 2007).
- [34] B. A. Kniehl and G. Kramer, Phys. Rev. D 74, 037502 (2006).
- [35] T. Kneesch, B. A. Kniehl, G. Kramer, and I. Schienbein, Nucl. Phys. B 799, 34 (2008).
- [36] J.-Q. Chen, *A New Apporach to Group Representations* (Shanghai Scientific and Technical Publishers, Shanghai, 1984).

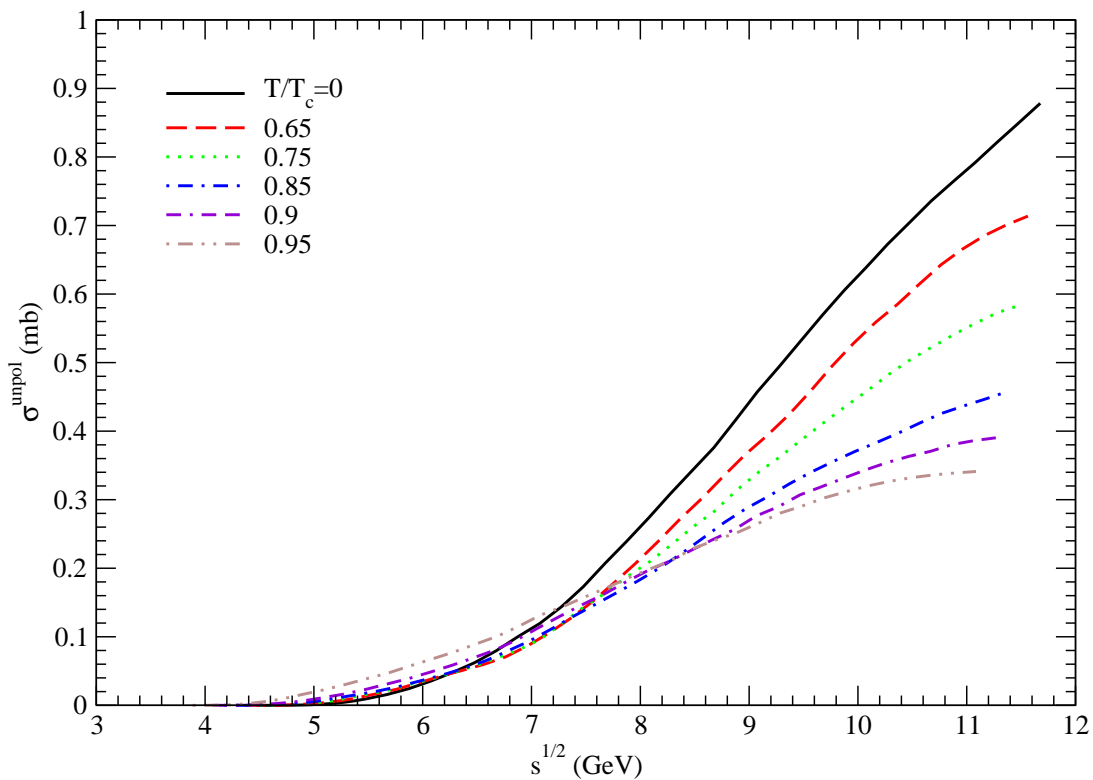


Figure 1: Cross sections for $\rho J/\psi \rightarrow D^+X + D^0X + D_s^+X + D^{*+}X$ at various temperatures.

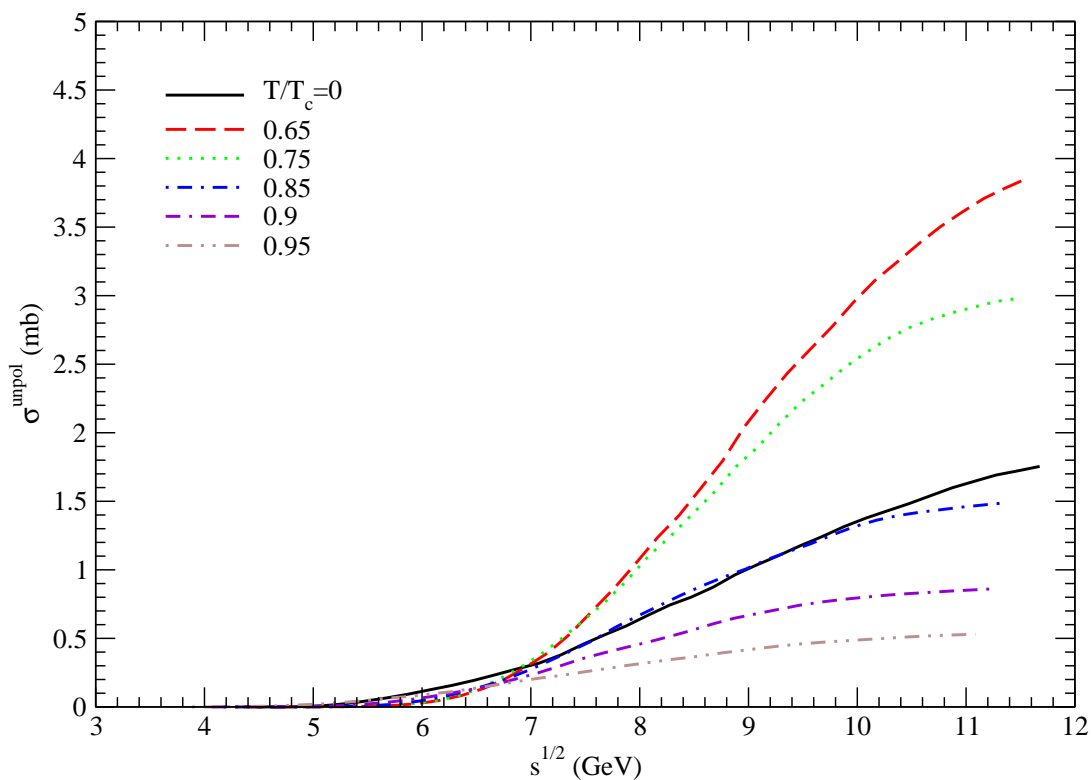


Figure 2: Cross sections for $\rho\psi' \rightarrow D^+X + D^0X + D_s^+X + D^{*+}X$ at various temperatures.

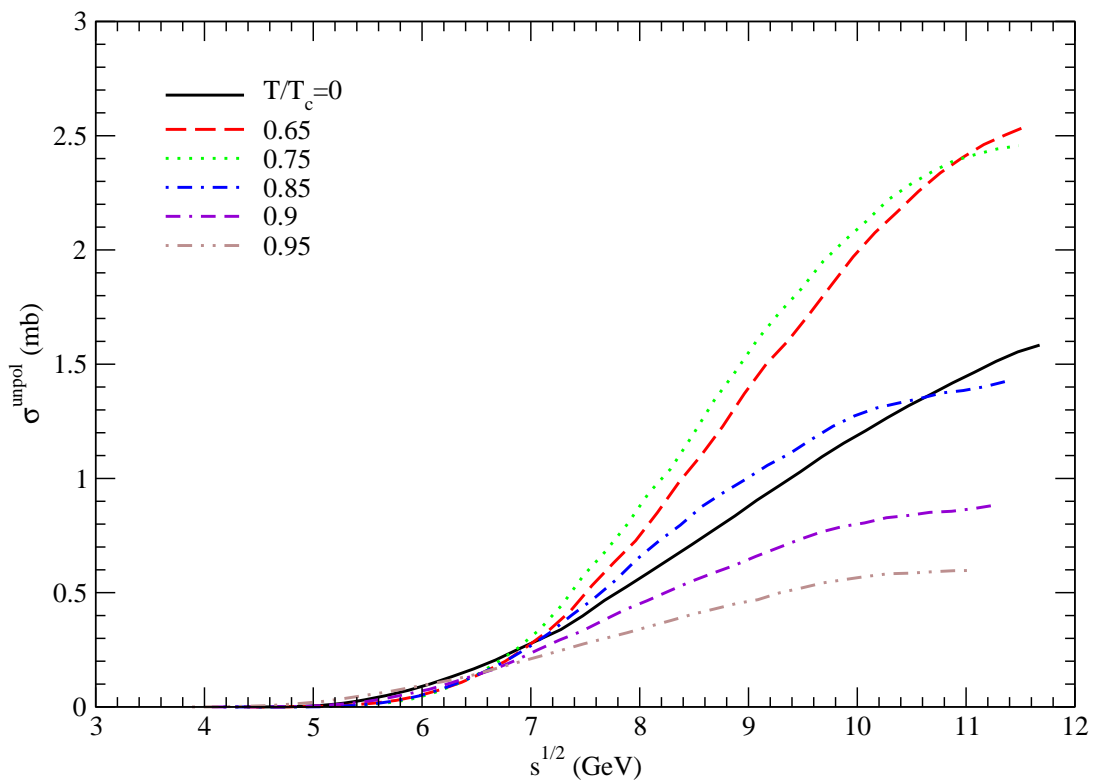


Figure 3: Cross sections for $\rho\chi_c \rightarrow D^+X + D^0X + D_s^+X + D^{*+}X$ at various temperatures.

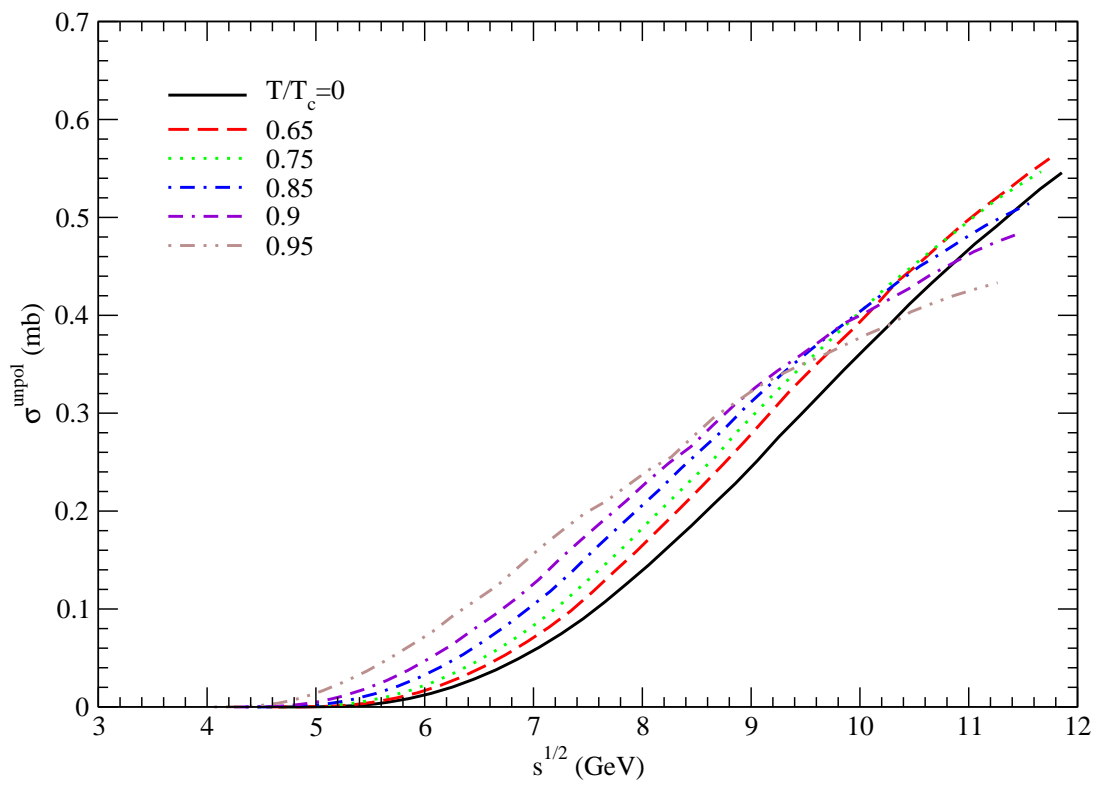


Figure 4: Cross sections for $KJ/\psi \rightarrow D^+X + D^0X + D_s^+X + D^{*+}X$ at various temperatures.

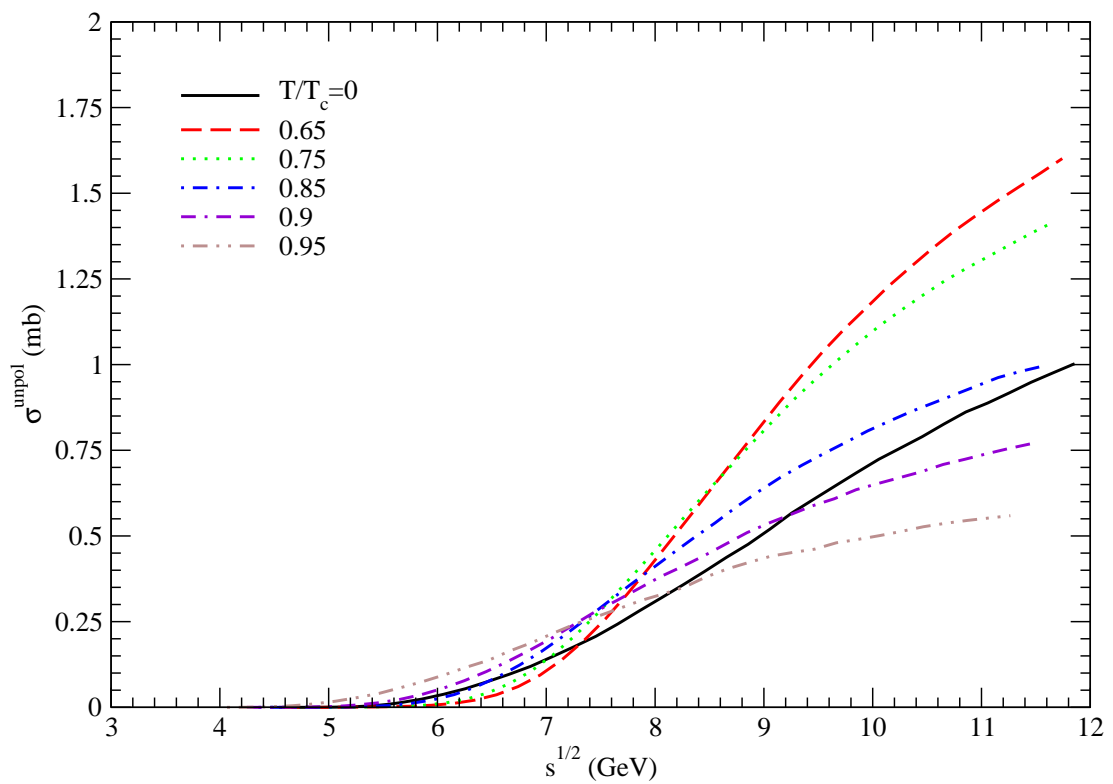


Figure 5: Cross sections for $K\psi' \rightarrow D^+X + D^0X + D_s^+X + D^{*+}X$ at various temperatures.

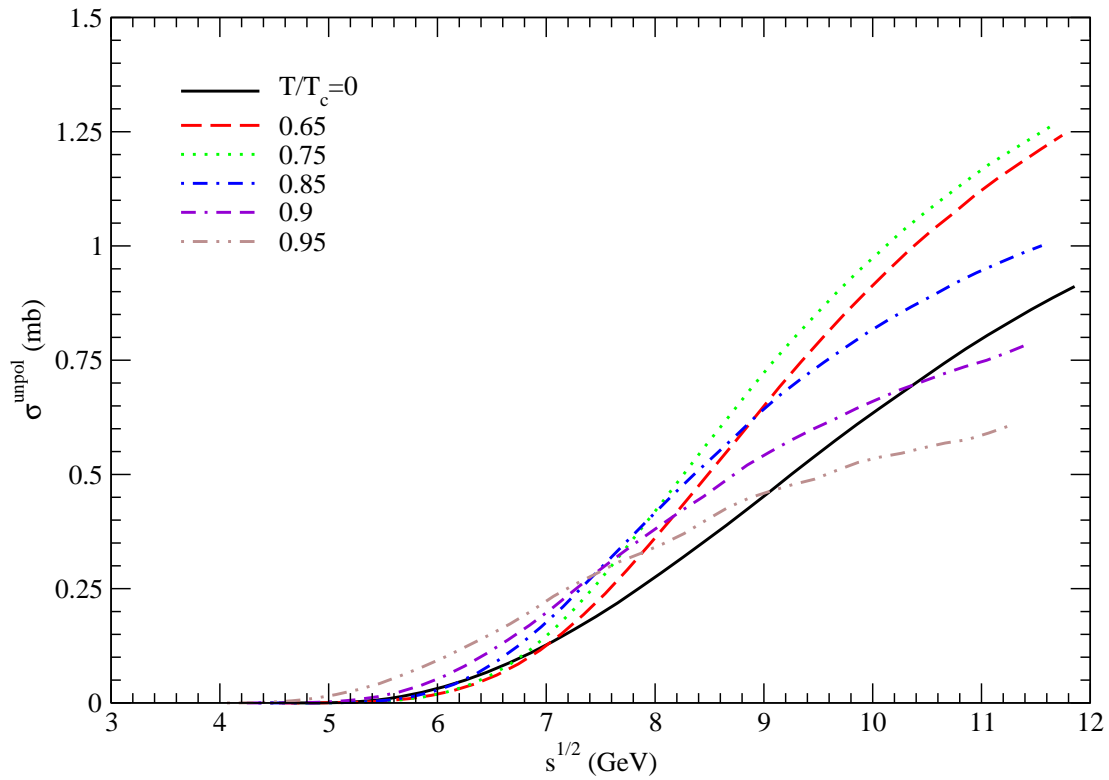


Figure 6: Cross sections for $K\chi_c \rightarrow D^+X + D^0X + D_s^+X + D^{*+}X$ at various temperatures.

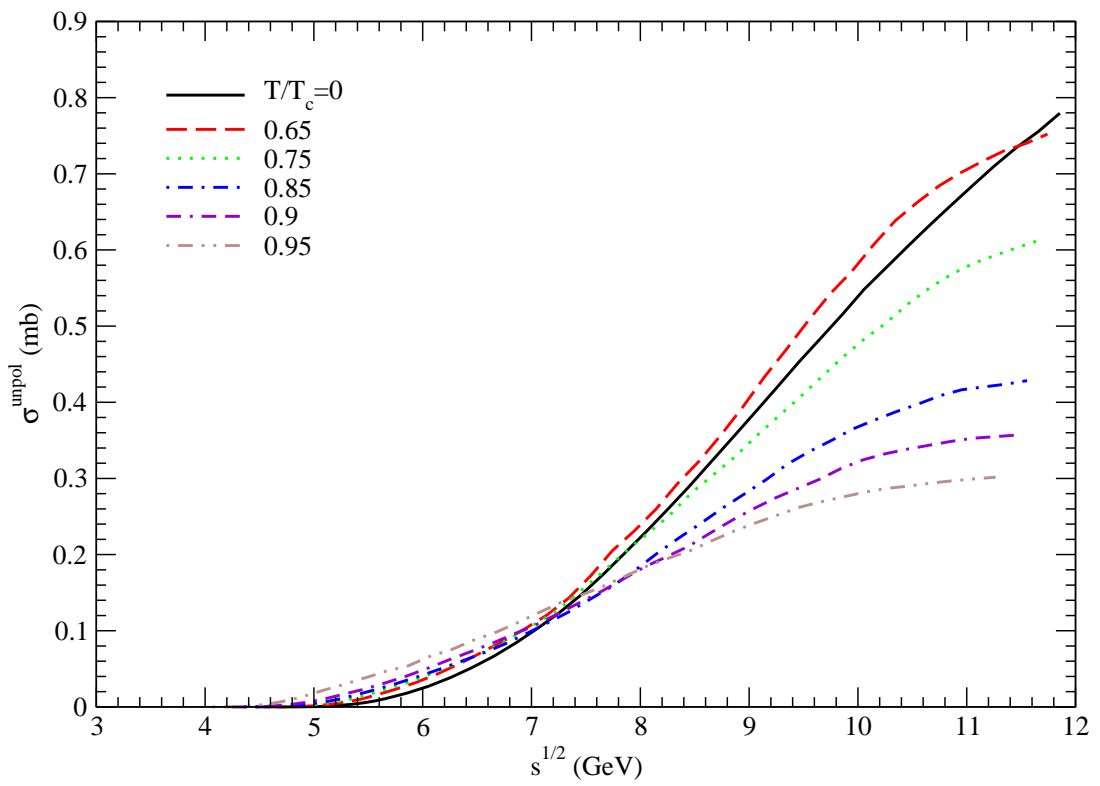


Figure 7: Cross sections for $K^*J/\psi \rightarrow D^+X + D^0X + D_s^+X + D^{*+}X$ at various temperatures.

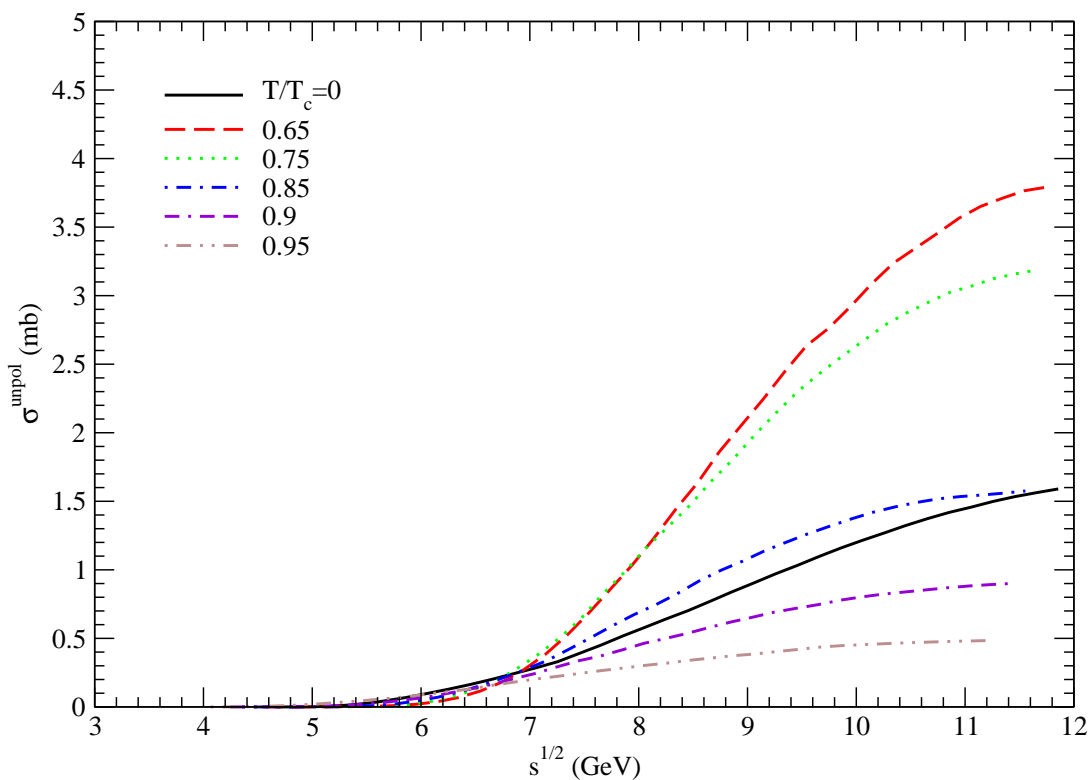


Figure 8: Cross sections for $K^*\psi' \rightarrow D^+X + D^0X + D_s^+X + D^{*+}X$ at various temperatures.

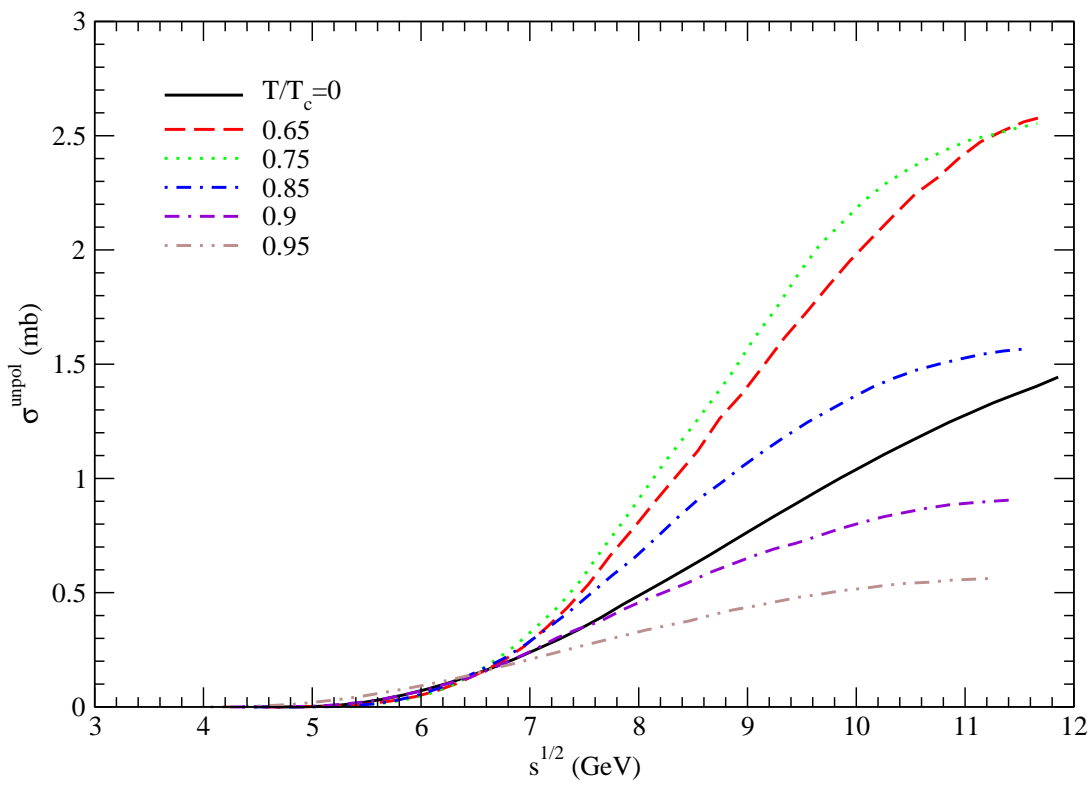


Figure 9: Cross sections for $K^*\chi_c \rightarrow D^+X + D^0X + D_s^+X + D^{*+}X$ at various temperatures.

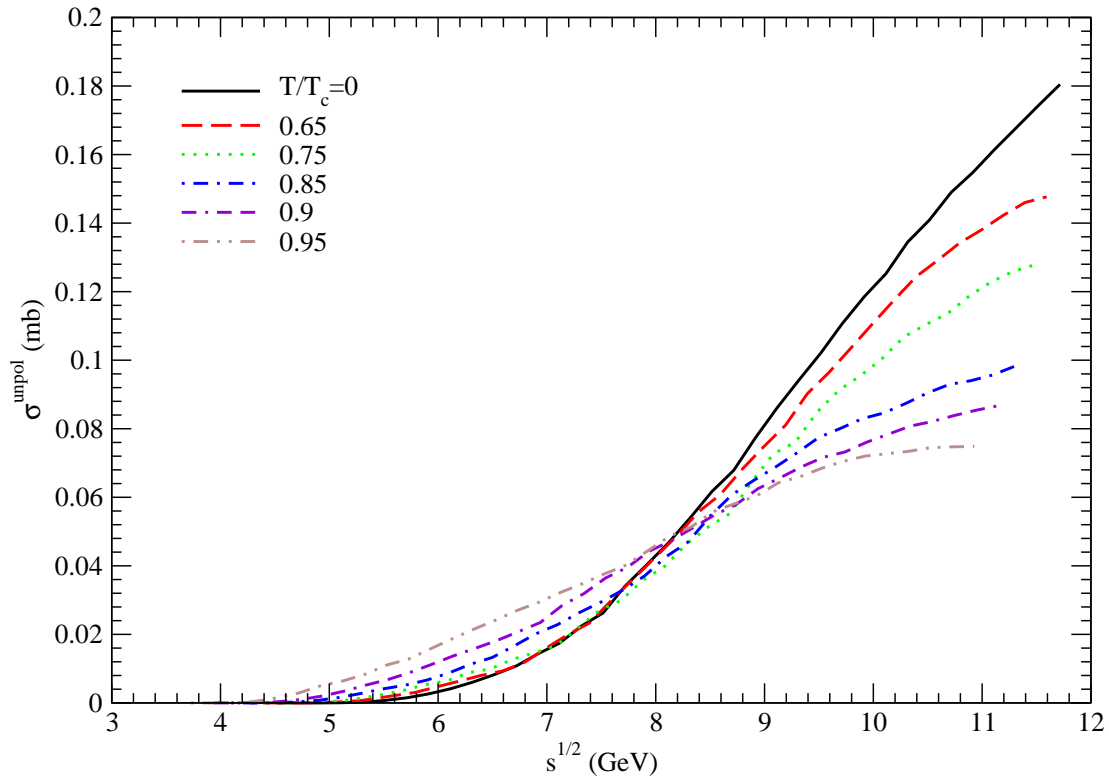


Figure 10: Cross sections for $\rho J/\psi \rightarrow D^{*+} X$ at various temperatures.

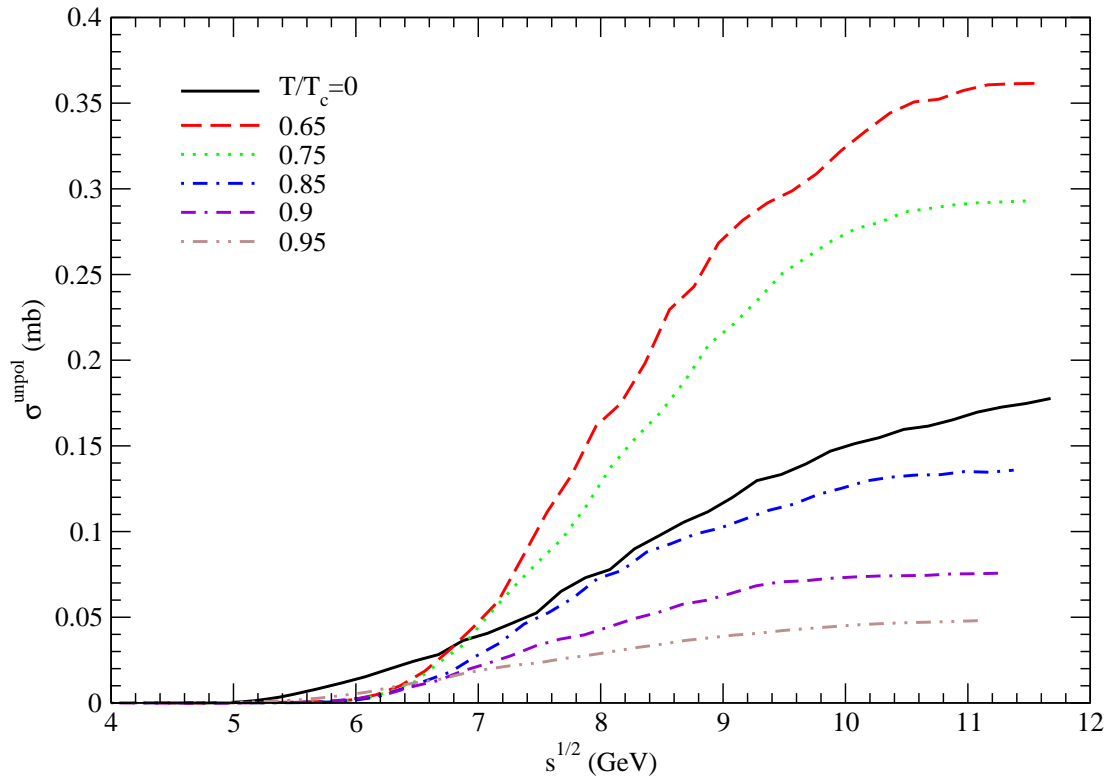


Figure 11: Cross sections for $\rho\psi' \rightarrow D_s^+ X$ at various temperatures.

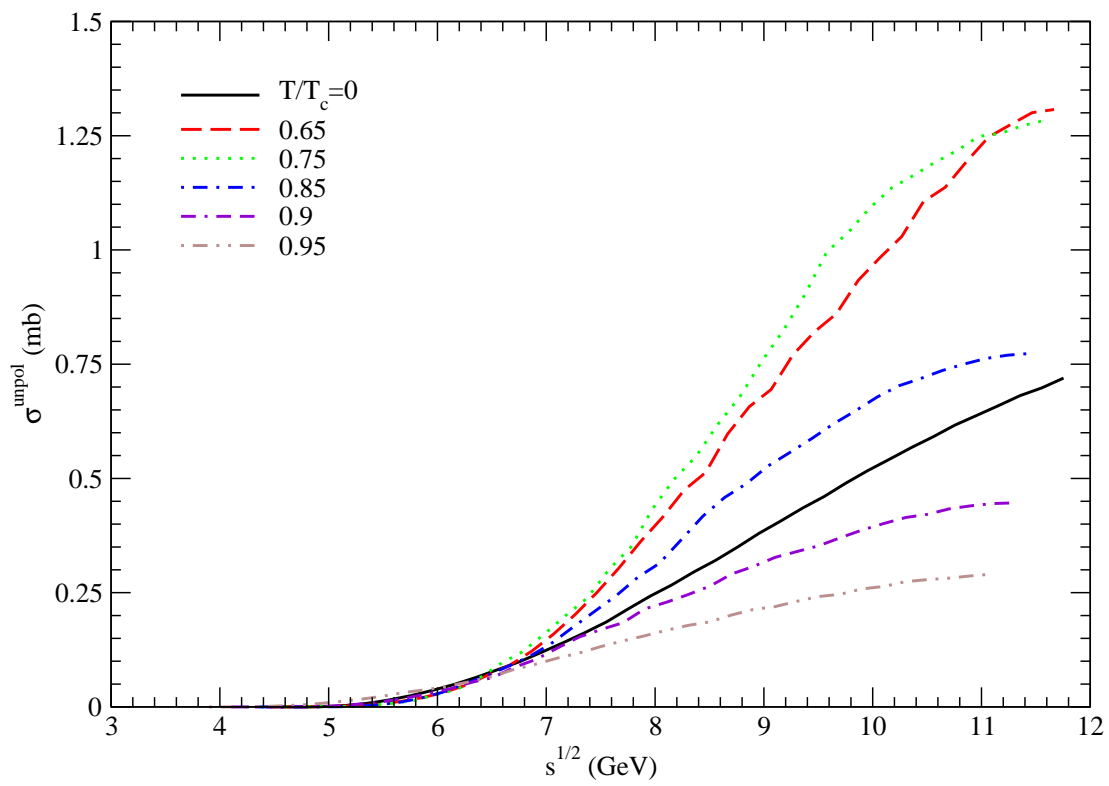


Figure 12: Cross sections for $K^*\chi_c \rightarrow D^0 X$ at various temperatures.

Table 1: Spin matrix elements

S_A	0	0	0	1	1	1	1	1	1
S_B	1	1	1	1	1	1	1	1	1
$S'_{q_1+\bar{q}_2}$	0	1	1	0	0	1	1	1	1
$S'_{c+\bar{c}}$	1	0	1	0	1	0	1	1	1
S	1	1	1	0	1	1	0	1	2
$\psi_{\text{final}}^{SS_z+}(\chi_A \chi_B)_{S_z}^S$	1	0	0	0	0	0	1	1	1
$\psi_{\text{final}}^{SS_z+} \vec{s}_{q_1} \cdot \vec{s}_{\bar{c}} (\chi_A \chi_B)_{S_z}^S$	0	$-\frac{1}{4}$	$-\frac{1}{2\sqrt{2}}$	$\frac{\sqrt{3}}{4}$	$-\frac{1}{2\sqrt{2}}$	$-\frac{1}{2\sqrt{2}}$	$-\frac{1}{2}$	$-\frac{1}{4}$	$\frac{1}{4}$
$\psi_{\text{final}}^{SS_z+} \vec{s}_{\bar{q}_2} \cdot \vec{s}_c (\chi_A \chi_B)_{S_z}^S$	0	$-\frac{1}{4}$	$\frac{1}{2\sqrt{2}}$	$\frac{\sqrt{3}}{4}$	$\frac{1}{2\sqrt{2}}$	$\frac{1}{2\sqrt{2}}$	$-\frac{1}{2}$	$-\frac{1}{4}$	$\frac{1}{4}$
$\psi_{\text{final}}^{SS_z+} \vec{s}_{q_1} \cdot \vec{s}_c (\chi_A \chi_B)_{S_z}^S$	0	$\frac{1}{4}$	$-\frac{1}{2\sqrt{2}}$	$-\frac{\sqrt{3}}{4}$	$-\frac{1}{2\sqrt{2}}$	$\frac{1}{2\sqrt{2}}$	$-\frac{1}{2}$	$-\frac{1}{4}$	$\frac{1}{4}$
$\psi_{\text{final}}^{SS_z+} \vec{s}_{\bar{q}_2} \cdot \vec{s}_{\bar{c}} (\chi_A \chi_B)_{S_z}^S$	0	$\frac{1}{4}$	$\frac{1}{2\sqrt{2}}$	$-\frac{\sqrt{3}}{4}$	$\frac{1}{2\sqrt{2}}$	$-\frac{1}{2\sqrt{2}}$	$-\frac{1}{2}$	$-\frac{1}{4}$	$\frac{1}{4}$

Table 2: Quantities relevant to the cross sections for the $\rho J/\psi$ dissociation reactions. a_1 and a_2 are in units of mb; b_1 , b_2 , d_0 , and $\sqrt{s_z}$ are in units of GeV; c_1 and c_2 are dimensionless.

Reaction	T/T_c	a_1	b_1	c_1	a_2	b_2	c_2	d_0	$\sqrt{s_z}$
$\rho + J/\psi \rightarrow D^+ + X$	0	0.02	4	4.1	0.16	8.3	6.2	8.11	27.19
	0.65	0.01	2.9	4.2	0.13	7.2	7.9	7.16	22.27
	0.75	0.006	2.5	4.4	0.106	7.7	5.7	7.69	26.2
	0.85	0.002	1.8	5.7	0.084	8.2	4.2	8.2	31.01
	0.9	0.002	2	5.1	0.082	8.7	3.8	8.7	33.94
	0.95	0.002	1.9	6.4	0.068	8.7	3.2	8.7	36.47
$\rho + J/\psi \rightarrow D^0 + X$	0	0.05	4	4.1	0.43	8.3	6.3	8.13	27.04
	0.65	0.02	2.4	5.3	0.34	7.6	6.8	7.6	24.45
	0.75	0.007	1.8	6.4	0.302	8.6	4.4	8.6	31.84
	0.85	0.003	1.5	9.7	0.23	8.8	3.7	8.8	34.83
	0.9	0.004	1.8	5.9	0.186	8	3.9	8	31.18
	0.95	0.008	1.9	5.9	0.162	7.6	3.9	7.6	29.61
$\rho + J/\psi \rightarrow D_s^+ + X$	0	0.007	3.1	4.6	0.084	7.3	5.7	7.23	25.32
	0.65	0.003	1.9	5.7	0.066	6.9	5.2	6.9	24.9
	0.75	0.01	3.4	4.2	0.051	6.7	8.9	6.51	20.21
	0.85	0.001	2	4.9	0.042	7.5	4.2	7.5	28.82
	0.9	0.001	2.9	4.5	0.038	7.8	4	7.78	30.31
	0.95	0.004	3.7	4.3	0.031	8	4.3	7.75	29.81
$\rho + J/\psi \rightarrow D^{*+} + X$	0	0.008	3.1	5.6	0.181	8	6.3	7.99	26.42
	0.65	0.002	1.7	7.2	0.156	8.5	4.8	8.5	30.63
	0.75	0.005	2.2	5.8	0.123	7.6	6	7.6	25.53
	0.85	0.05	7.2	10.4	0.05	7.4	3	7.24	30.58
	0.9	0.003	1.9	5.8	0.086	7.9	3.8	7.9	31.2
	0.95	0.002	1.6	7.8	0.071	7.5	3.1	7.5	32.44

Table 3: The same as Table 2 except for $\rho\psi'$.

Reaction	T/T_c	a_1	b_1	c_1	a_2	b_2	c_2	d_0	$\sqrt{s_z}$
$\rho + \psi' \rightarrow D^+ + X$	0	0.01	1.7	5.3	0.347	8.4	3.6	8.4	34.23
	0.65	0.1	5	9	0.7	8.2	6.4	7.88	26.51
	0.75	0.2	5	9	0.6	9.7	7.3	9.3	29.13
	0.85	0.02	3.2	12.5	0.28	7.3	6.8	7.3	23.42
	0.9	0.003	2.5	12.9	0.162	6.9	5.5	6.9	23.96
	0.95	0.002	2	4.9	0.098	7.3	4	7.3	28.28
$\rho + \psi' \rightarrow D^0 + X$	0	0.1	2.9	3.8	0.816	7.1	6.6	7.01	23.5
	0.65	0.2	5	8	1.8	7.9	7	7.67	24.92
	0.75	0.11	3.9	19.2	1.71	8.3	6.2	8.3	27.08
	0.85	0.11	3.9	9.2	0.72	7	9.2	6.86	20.54
	0.9	0.02	3	8	0.42	6.8	6.3	6.79	22.54
	0.95	0.01	2.6	3.9	0.26	7.6	4.2	7.58	28.69
$\rho + \psi' \rightarrow D_s^+ + X$	0	0.01	2	5.1	0.17	6.9	4.7	6.9	25.98
	0.65	0.12	4.2	12	0.332	7.1	10.3	6.72	20.37
	0.75	0.04	3.4	19.6	0.299	6.4	9.9	6.39	18.98
	0.85	0.022	3.3	20.6	0.139	6.2	10.4	6.19	18.16
	0.9	0.011	3.3	21.1	0.077	6.4	7.7	6.39	20.22
	0.95	0.005	3.2	12.8	0.048	6.9	5.3	6.89	24.25
$\rho + \psi' \rightarrow D^{*+} + X$	0	0.01	2	6.5	0.35	7.7	5	7.7	27.84
	0.65	0.031	3.5	29.8	0.79	6.9	9.7	6.9	20.36
	0.75	0.11	3.9	14.7	0.61	6.6	15	6.52	17.47
	0.85	0.07	4.2	10.5	0.33	7.9	6.7	7.7	25.15
	0.9	0.01	3	13	0.18	6.6	5.4	6.59	23.26
	0.95	0.01	3.5	3.9	0.11	7.8	3.5	7.6	31.72

Table 4: The same as Table 2 except for $\rho\chi_c$.

Reaction	T/T_c	a_1	b_1	c_1	a_2	b_2	c_2	d_0	$\sqrt{s_z}$
$\rho + \chi_c \rightarrow D^+ + X$	0	0.01	2.3	4.1	0.31	8.5	3.9	8.5	33.33
	0.65	0.014	2.5	9.6	0.451	7.1	7	7.1	22.9
	0.75	0.1	6	6	0.4	8.1	5.8	7.62	26.8
	0.85	0.02	4	9	0.28	7.7	5.6	7.62	26.22
	0.9	0.02	4	7	0.18	8.7	4.7	8.59	31.02
	0.95	0.002	2	7.4	0.121	8.3	3.6	8.3	33.14
$\rho + \chi_c \rightarrow D^0 + X$	0	0.1	4	3.4	0.96	10.2	4.3	10.03	37.47
	0.65	0.01	7	2	1.25	8.1	5.1	8.1	28.75
	0.75	0.1	3.8	8.4	1.3	7.5	7.5	7.44	23.31
	0.85	0.1	4.1	7.5	0.7	7.5	7.8	7.33	22.85
	0.9	0.01	3	10	0.4	7.2	5	7.2	25.74
	0.95	0.02	3	4	0.3	7.8	4.7	7.74	28.02
$\rho + \chi_c \rightarrow D_s^+ + X$	0	0.01	3	4.1	0.16	8	3.8	7.94	32.07
	0.65	0.005	5	2.9	0.232	6.5	6	6.48	22.57
	0.75	0.014	3.9	15	0.247	6.4	7.1	6.34	20.96
	0.85	0.02	3.4	16.1	0.14	6.4	8.8	6.37	19.52
	0.9	0.01	3.5	17.1	0.08	6.4	7.2	6.36	20.65
	0.95	0.013	3.7	8.8	0.049	7.1	7.1	6.85	22.35
$\rho + \chi_c \rightarrow D^{*+} + X$	0	0.01	2.6	5.6	0.33	8.1	4.9	8.1	29.28
	0.65	0.1	5.5	11.4	0.6	10.1	4.9	9.8	35.23
	0.75	0.1	4.9	8.4	0.5	7.6	8.4	7.25	22.7
	0.85	0.012	3.1	13.1	0.305	6.3	7.3	6.29	20.34
	0.9	0.01	2.7	11.2	0.192	6.9	5.3	6.9	24.3
	0.95	0.03	3.4	4.4	0.12	7.1	7	6.81	22.25

Table 5: The same as Table 2 except for KJ/ψ .

Reaction	T/T_c	a_1	b_1	c_1	a_2	b_2	c_2	d_0	$\sqrt{s_z}$
$K + J/\psi \rightarrow D^+ + X$	0	0.01	0.01	0.08	0.11	9.13	3.77	9.13	36.18
	0.65	0.01	0.01	0.07	0.11	8.83	3.8	8.83	34.93
	0.75	0.01	0.01	0.08	0.105	8.71	3.68	8.71	34.91
	0.85	0.01	0.01	0.09	0.097	8.42	3.57	8.42	34.21
	0.9	0.01	0.01	0.07	0.088	7.99	3.46	7.99	33
	0.95	0.01	2.9	4.4	0.08	7.7	4.7	7.62	27.88
$K + J/\psi \rightarrow D^0 + X$	0	0.01	0.01	0.06	0.28	9	3.85	9	35.41
	0.65	0.01	0.01	0.05	0.28	8.73	3.87	8.73	34.32
	0.75	0.01	0.01	0.09	0.29	9.13	3.64	9.13	36.56
	0.85	0.01	0.01	0.08	0.26	8.62	3.58	8.62	34.88
	0.9	0.01	0.01	0.08	0.24	8.39	3.41	8.39	34.67
	0.95	0.02	2.9	4.4	0.22	8.3	4	8.25	31.82
$K + J/\psi \rightarrow D_s^+ + X$	0	0.01	0.01	0.08	0.05	7.38	4.05	7.38	29.34
	0.65	0.01	0.01	0.07	0.06	8.12	3.69	8.12	32.97
	0.75	0.01	0.01	0.09	0.05	7.25	3.84	7.25	29.35
	0.85	0.01	4.4	4.6	0.05	9.4	4.1	8.9	35.48
	0.9	0.01	4.1	4.7	0.04	8	5.3	7.48	27.69
	0.95	0.01	3.7	5.1	0.04	8.7	4.9	8.41	30.61
$K + J/\psi \rightarrow D^{*+} + X$	0	0.01	0.01	0.09	0.11	8.5	4.5	8.5	31.73
	0.65	0.01	0.01	0.07	0.12	8.43	4.32	8.43	31.91
	0.75	0.01	0.01	0.13	0.12	8.45	4.04	8.45	32.76
	0.85	0.01	0.01	0.1	0.107	7.76	3.71	7.76	31.37
	0.9	0.01	0.01	0.09	0.099	7.35	3.42	7.35	30.86
	0.95	0.01	2.5	4.7	0.09	7.1	4.2	7.06	27.23

Table 6: The same as Table 2 except for $K\psi'$.

Reaction	T/T_c	a_1	b_1	c_1	a_2	b_2	c_2	d_0	$\sqrt{s_z}$
$K + \psi' \rightarrow D^+ + X$	0	0.01	0.01	0.08	0.18	8.02	3.69	8.02	32.63
	0.65	0.01	0.01	0.03	0.28	6.78	7.22	6.78	22.02
	0.75	0.1	4.8	9	0.243	8.47	9.6	7.9	23.92
	0.85	0.02	3.7	10	0.188	7.8	5.8	7.76	26.36
	0.9	0.02	4	7	0.15	8.7	4.5	8.55	31.75
	0.95	0.02	4.2	3.8	0.1	8.7	4	8.15	32.99
$K + \psi' \rightarrow D^0 + X$	0	0.01	0.01	0.06	0.48	8.19	3.69	8.19	33.23
	0.65	0.01	0.01	0.02	0.73	6.81	7.26	6.81	22.06
	0.75	0.14	4.3	10	0.705	8.13	7.67	7.96	24.9
	0.85	0.1	4.2	8	0.481	8.1	6.9	7.86	25.55
	0.9	0.1	4.7	6	0.44	10.6	4.4	10.25	38.11
	0.95	0.01	3	6	0.3	8.6	3.3	8.59	35.76
$K + \psi' \rightarrow D_s^+ + X$	0	0.01	0.01	0.08	0.1	7.48	3.63	7.48	31.06
	0.65	0.05	4.2	13.6	0.15	7.6	7.5	7.34	23.89
	0.75	0.03	3.7	19	0.133	6.83	7.67	6.79	21.72
	0.85	0.017	3.4	20	0.091	6.6	7.5	6.59	21.18
	0.9	0.014	3.5	15	0.067	6.9	6.4	6.86	23.01
	0.95	0.02	4.1	6.6	0.05	8.6	6.4	8.1	27.36
$K + \psi' \rightarrow D^{*+} + X$	0	0.01	2.6	6.4	0.2	7.7	5.7	7.7	26.7
	0.65	0.1	5	14	0.47	10.4	6.5	10.36	32.68
	0.75	0.05	4.1	18	0.318	7.94	7.41	7.92	24.81
	0.85	0.047	3.9	10	0.211	7.6	7.1	7.44	24.06
	0.9	0.04	4	7	0.18	9.2	4.4	9.01	33.66
	0.95	0.03	4	4	0.12	9.3	3.5	8.65	37.19

Table 7: The same as Table 2 except for $K\chi_c$.

Reaction	T/T_c	a_1	b_1	c_1	a_2	b_2	c_2	d_0	$\sqrt{s_z}$
$K + \chi_c \rightarrow D^+ + X$	0	0.01	0.01	0.06	0.18	8.93	3.37	8.93	37.29
	0.65	0.01	0.01	0.05	0.23	7.6	4.98	7.6	27.53
	0.75	0.1	5.5	6.4	0.273	11.4	5.8	10.65	36.57
	0.85	0.03	4	8	0.183	7.9	6.2	7.72	25.98
	0.9	0.02	4	6.7	0.15	8.6	4.5	8.43	31.43
	0.95	0.01	3.6	5	0.12	9	3.3	8.9	37.23
$K + \chi_c \rightarrow D^0 + X$	0	0.01	0.01	0.05	0.46	8.85	3.42	8.85	36.75
	0.65	0.01	0.01	0.04	0.59	7.59	5.04	7.59	27.38
	0.75	0.1	4.7	8.1	0.695	9.51	4.97	9.31	33.23
	0.85	0.1	4.4	8	0.519	9.1	5.3	8.89	31.06
	0.9	0.1	4.3	5.9	0.37	8.4	6.5	7.96	26.69
	0.95	0.1	5.1	4	0.4	14	3.2	13.51	56.52
$K + \chi_c \rightarrow D_s^+ + X$	0	0.01	0.01	0.08	0.09	7.6	3.52	7.6	31.9
	0.65	0.01	0.01	0.06	0.12	6.59	5.26	6.59	24.06
	0.75	0.013	3.6	18	0.12	6.9	5.8	6.88	24.04
	0.85	0.032	3.9	12	0.089	7.4	8.2	7.2	22.55
	0.9	0.02	3.7	11.3	0.07	7.3	7.5	7.17	22.85
	0.95	0.01	3.2	9.5	0.05	6.7	6.2	6.61	22.52
$K + \chi_c \rightarrow D^{*+} + X$	0	0.01	0.01	0.08	0.18	8.29	4.11	8.29	32.22
	0.65	0.01	0.01	0.06	0.28	8.15	5.44	8.15	28.35
	0.75	0.1	5.3	8.4	0.303	10.92	5.49	10.46	36.12
	0.85	0.05	4	9	0.207	7.6	7.1	7.35	24.04
	0.9	0.03	3.8	7.2	0.17	8.2	4.5	8.01	30.17
	0.95	0.02	3.7	4.6	0.13	8.7	3.2	8.39	36.6

Table 8: The same as Table 2 except for K^*J/ψ .

Reaction	T/T_c	a_1	b_1	c_1	a_2	b_2	c_2	d_0	$\sqrt{s_z}$
$K^* + J/\psi \rightarrow D^+ + X$	0	0.01	3	4.4	0.15	8.3	5	8.27	29.69
	0.65	0.009	2.5	4.3	0.154	8.1	5.4	8.09	28.17
	0.75	0.01	2.7	4	0.12	7.9	5.6	7.87	27.13
	0.85	0.002	1.6	6.6	0.083	8.6	3.4	8.6	35.62
	0.9	0.01	2.8	4.1	0.07	7.1	6.5	7.01	23.27
	0.95	0.003	2	6	0.062	8.6	2.9	8.6	38.01
$K^* + J/\psi \rightarrow D^0 + X$	0	0.1	6	3.4	0.41	11.3	4.3	10.43	40.86
	0.65	0.01	1.8	5.6	0.39	8.3	4.3	8.3	31.44
	0.75	0.01	1.9	4.8	0.31	8.2	4.2	8.2	31.32
	0.85	0.01	2	5	0.22	8.1	4.1	8.1	31.17
	0.9	0.03	3.1	3.9	0.17	7.2	7.1	7.05	22.83
	0.95	0.004	1.5	8	0.14	7.4	3.1	7.4	32.23
$K^* + J/\psi \rightarrow D_s^+ + X$	0	0.02	4.3	4.1	0.07	8.2	6.5	7.7	26.61
	0.65	0.005	2.3	4.2	0.073	6.9	4.9	6.88	25.64
	0.75	0.007	3.2	3.5	0.057	7.8	4.3	7.62	29.76
	0.85	0.001	2	5.5	0.046	8	3.4	8	33.55
	0.9	0.004	2.6	5.1	0.031	6.9	5.3	6.85	24.6
	0.95	0.006	3	4.8	0.024	6.6	6.8	6.38	21.52
$K^* + J/\psi \rightarrow D^{*+} + X$	0	0.03	4.7	4.6	0.15	8.4	7.5	8.07	25.97
	0.65	0.007	2.5	4.9	0.147	7.4	5.8	7.39	25.56
	0.75	0.01	2.7	4.7	0.12	7.2	6.2	7.17	24.31
	0.85	0.003	1.7	6.6	0.094	7.7	3.7	7.7	31.2
	0.9	0.002	1.7	7.4	0.079	7.8	3	7.8	34.5
	0.95	0.003	1.5	9.6	0.062	6.8	3	6.8	30.39

Table 9: The same as Table 2 except for $K^*\psi'$.

Reaction	T/T_c	a_1	b_1	c_1	a_2	b_2	c_2	d_0	$\sqrt{s_z}$
$K^* + \psi' \rightarrow D^+ + X$	0	0.01	2	5.1	0.31	8.4	3.5	8.4	34.78
	0.65	0.2	5.2	8.9	0.7	9.6	5.2	8.87	32.91
	0.75	0.1	4	9.5	0.6	7.5	8.1	7.36	22.91
	0.85	0.02	3	11	0.28	6.7	6.8	6.69	22.01
	0.9	0.002	2.2	11.2	0.164	6.9	4.8	6.9	25.4
	0.95	0.01	6	3	0.09	8.6	2.9	8.28	37.66
$K^* + \psi' \rightarrow D^0 + X$	0	0.1	2.9	4.2	0.78	7.5	6	7.42	25.53
	0.65	0.08	3.5	24	1.91	7.5	6.3	7.5	25
	0.75	0.2	3.8	9.8	1.6	7.1	8.7	7.01	21.46
	0.85	0.1	3.3	9.5	0.8	6.9	8.5	6.86	21
	0.9	0.01	3	10	0.44	7.5	4.4	7.5	28.21
	0.95	0.001	1.2	7.7	0.229	7.3	3.2	7.3	31.38
$K^* + \psi' \rightarrow D_s^+ + X$	0	0.005	1.7	6	0.151	7.1	3.7	7.1	29.48
	0.65	0.08	4	14	0.36	7	6.9	6.79	22.97
	0.75	0.06	3.5	15.7	0.31	6.5	8.8	6.45	20.04
	0.85	0.031	3.4	15.8	0.145	6.4	8.9	6.36	19.63
	0.9	0.009	3.1	16.7	0.083	6.4	6.9	6.39	21.12
	0.95	0.005	3.1	7.5	0.042	6.7	5.1	6.62	24.17
$K^* + \psi' \rightarrow D^{*+} + X$	0	0.01	2	6.3	0.32	7.7	4.7	7.7	28.69
	0.65	0.3	4.9	11.5	0.8	8	12.8	7.58	21.3
	0.75	0.1	4.2	16.3	0.7	7.5	7.5	7.43	23.58
	0.85	0.08	4	9	0.37	7.9	6.7	7.72	25.33
	0.9	0.04	4	6	0.17	7.5	4.8	6.96	27.12
	0.95	0.003	1.9	7.2	0.109	7.3	3	7.3	32.34

Table 10: The same as Table 2 except for $K^*\chi_c$.

Reaction	T/T_c	a_1	b_1	c_1	a_2	b_2	c_2	d_0	$\sqrt{s_z}$
$K^* + \chi_c \rightarrow D^+ + X$	0	0.02	3	3.5	0.3	9.1	3.9	9.05	35.54
	0.65	0.004	2	6.6	0.472	7.5	5.1	7.5	26.98
	0.75	0.1	5.5	7.4	0.4	8.2	4.7	7.4	29.57
	0.85	0.009	2.6	12.4	0.277	6.7	6	6.7	22.97
	0.9	0.01	3	7.3	0.18	7.8	4.6	7.79	28.66
	0.95	0.01	3.1	3.6	0.11	8.4	3.8	8.3	32.86
$K^* + \chi_c \rightarrow D^0 + X$	0	0.1	4.1	3.2	0.88	10.7	3.9	10.49	40.95
	0.65	0.02	6.7	2.1	1.23	7.7	4.9	7.69	28.24
	0.75	0.1	3.8	6.8	1.3	7.6	6.3	7.52	25.17
	0.85	0.02	2.4	14.9	0.75	6.9	5.9	6.9	23.67
	0.9	0.04	4.7	7.7	0.43	8	4	7.7	30.94
	0.95	0.01	4	3	0.29	8.7	3.1	8.59	37.16
$K^* + \chi_c \rightarrow D_s^+ + X$	0	0.02	3.3	3.8	0.14	8.1	4.2	7.9	31.22
	0.65	0.01	5	3	0.24	6.3	5.7	6.27	22.62
	0.75	0.04	4	10	0.25	6.9	6.1	6.64	23.57
	0.85	0.018	3.1	17.5	0.152	6.3	7.7	6.29	20.25
	0.9	0.02	3.4	11.2	0.08	6.4	9.6	6.28	19.09
	0.95	0.006	3.1	9.4	0.048	6.6	5.3	6.55	23.54
$K^* + \chi_c \rightarrow D^{*+} + X$	0	0.01	2.7	5.2	0.31	8.6	4.3	8.6	32.64
	0.65	0.1	4.8	13.7	0.95	12.9	4	12.9	47.98
	0.75	0.1	4.7	10	0.5	8	5.9	7.56	26.9
	0.85	0.04	3.5	9.8	0.337	7.1	6.3	7.04	23.71
	0.9	0.02	3	6	0.19	6.7	5.9	6.63	22.97
	0.95	0.01	2.8	4.1	0.12	7.8	3.2	7.73	33.26

Table 11: The same as Table 2 except for $\pi J/\psi$.

Reaction	T/T_c	a_1	b_1	c_1	a_2	b_2	c_2	d_0	$\sqrt{s_z}$
$\pi + J/\psi \rightarrow D^+ + X$	0	0.01	0.01	0.09	0.12	9.27	4.18	9.27	34.91
	0.65	0.01	0.01	0.09	0.12	9.17	4.16	9.17	34.56
	0.75	0.01	0.01	0.1	0.11	8.67	4.16	8.67	32.82
	0.85	0.01	0.01	0.09	0.102	8.23	4.12	8.23	31.36
	0.9	0.01	0.01	0.11	0.099	8.08	3.93	8.08	31.35
	0.95	0.01	3.2	4.9	0.1	8.3	4.6	8.24	29.84
$\pi + J/\psi \rightarrow D^0 + X$	0	0.01	0.01	0.09	0.3	9.15	4.23	9.15	34.34
	0.65	0.01	0.01	0.09	0.31	9.13	4.2	9.13	34.29
	0.75	0.01	0.01	0.08	0.3	8.92	4.16	8.92	33.65
	0.85	0.01	3.1	5.4	0.29	8.6	4.7	8.59	30.86
	0.9	0.01	0.01	0.09	0.27	8.33	3.93	8.33	32.19
	0.95	0.02	3	5	0.26	8.1	4.6	8.07	29.21
$\pi + J/\psi \rightarrow D_s^+ + X$	0	0.01	0.01	0.1	0.06	7.98	4.41	7.98	30.1
	0.65	0.01	0.01	0.1	0.06	7.87	4.24	7.87	30.11
	0.75	0.01	4.5	5.1	0.06	9.5	4.5	9.14	34.41
	0.85	0.01	4.1	5.4	0.05	8	6.2	7.67	26.13
	0.9	0.01	4.2	5.7	0.05	8.7	5.2	8.36	29.88
	0.95	0.006	3.5	6.3	0.044	7.6	5	7.46	26.88
$\pi + J/\psi \rightarrow D^{*+} + X$	0	0.01	0.01	0.1	0.12	8.58	5.01	8.58	30.48
	0.65	0.01	0.01	0.09	0.12	8.3	4.85	8.3	29.89
	0.75	0.01	3.6	5.9	0.12	7.9	6.7	7.84	25.35
	0.85	0.02	4.5	4.8	0.13	9.4	5	9.09	32.49
	0.9	0.01	3.5	4.9	0.12	8.3	4.4	8.21	30.6
	0.95	0.01	3	5.1	0.11	7.8	4	7.74	29.96

Table 12: The same as Table 2 except for $\pi\psi'$.

Reaction	T/T_c	a_1	b_1	c_1	a_2	b_2	c_2	d_0	$\sqrt{s_z}$
$\pi + \psi' \rightarrow D^+ + X$	0	0.01	0.01	0.08	0.17	8.07	4	8.07	31.53
	0.65	0.01	0.01	0.03	0.25	6.97	7.64	6.97	21.93
	0.75	0.03	4.2	13	0.246	8.2	6.9	8.15	25.82
	0.85	0.017	3.8	11	0.172	7.7	6.5	7.66	24.86
	0.9	0.05	4.9	6.4	0.17	10.6	6	10.21	33.48
	0.95	0.01	3.7	5.1	0.12	8.5	4	8.38	32.3
$\pi + \psi' \rightarrow D^0 + X$	0	0.01	0.01	0.06	0.44	8.04	4.06	8.04	31.23
	0.65	0.01	0.01	0.02	0.64	6.91	7.88	6.91	21.57
	0.75	0.05	4	14	0.614	7.7	7.2	7.67	24.15
	0.85	0.05	4	10	0.458	7.9	6.6	7.83	25.26
	0.9	0.1	4.5	6.7	0.36	8.4	7.6	7.98	25.12
	0.95	0.1	4.8	4.5	0.31	9.7	5.6	8.95	31.43
$\pi + \psi' \rightarrow D_s^+ + X$	0	0.01	0.01	0.06	0.09	7.26	4.05	7.26	28.76
	0.65	0.03	4.1	18.7	0.14	7.5	7.3	7.44	23.69
	0.75	0.023	3.8	24	0.117	6.9	7.9	6.88	21.52
	0.85	0.021	3.8	19.5	0.091	7.6	7.1	7.59	23.98
	0.9	0.018	3.9	15.1	0.073	8.1	6.2	8.07	26.39
	0.95	0.02	4.2	8.3	0.07	10.5	4.9	10.44	35.98
$\pi + \psi' \rightarrow D^{*+} + X$	0	0.01	0.01	0.01	0.19	8.13	4.8	8.13	29.61
	0.65	0.09	5	16.7	0.82	14.2	5.7	14.2	44.98
	0.75	0.095	4.9	14.5	0.732	14.3	5.7	14.3	45.15
	0.85	0.031	3.9	13	0.202	7.7	6.7	7.65	24.64
	0.9	0.03	3.8	7.7	0.16	7.7	6.1	7.52	25.28
	0.95	0.03	4	4.9	0.15	9.8	3.8	9.52	37.49

Table 13: The same as Table 2 except for $\pi\chi_c$.

Reaction	T/T_c	a_1	b_1	c_1	a_2	b_2	c_2	d_0	$\sqrt{s_z}$
$\pi + \chi_c \rightarrow D^+ + X$	0	0.01	0.01	0.1	0.17	8.86	3.72	8.86	35.27
	0.65	0.01	0.01	0.06	0.21	7.83	5.29	7.83	27.41
	0.75	0.05	5	7.2	0.21	8.8	6.9	8.32	27.27
	0.85	0.02	4	10	0.18	8.2	6	8.14	26.97
	0.9	0.03	4.4	6.7	0.15	9	5.6	8.71	29.79
	0.95	0.01	3.8	5.8	0.13	8.8	3.8	8.71	34.07
$\pi + \chi_c \rightarrow D^0 + X$	0	0.01	0.01	0.07	0.45	8.98	3.75	8.98	35.56
	0.65	0.01	0.01	0.05	0.54	7.85	5.33	7.85	27.39
	0.75	0.1	5	9	0.68	10.3	5	10.14	35.38
	0.85	0.12	4.7	8	0.495	9.2	6.9	8.9	28.26
	0.9	0.1	4.7	6.5	0.41	9.6	5.8	9.21	31.07
	0.95	0.1	5	4.5	0.36	11	4.4	10.26	38.89
$\pi + \chi_c \rightarrow D_s^+ + X$	0	0.01	0.01	0.09	0.09	7.74	3.93	7.74	30.74
	0.65	0.01	0.01	0.06	0.11	6.6	5.85	6.6	23.01
	0.75	0.01	3.6	19	0.109	6.94	6.42	6.93	23.14
	0.85	0.02	3.8	15	0.085	7.1	8.2	7.02	21.65
	0.9	0.02	3.9	12.7	0.07	7.6	7.7	7.49	23.23
	0.95	0.02	3.9	9.3	0.06	8	7.6	7.81	24.15
$\pi + \chi_c \rightarrow D^{*+} + X$	0	0.01	0.01	0.08	0.17	8.09	4.64	8.09	29.88
	0.65	0.01	0.01	0.07	0.23	7.96	5.92	7.96	26.77
	0.75	0.08	5.3	9.8	0.377	12.5	5.2	12.45	41.48
	0.85	0.027	3.8	11.6	0.199	7.5	6.9	7.44	23.87
	0.9	0.03	3.9	7.9	0.17	8.2	5.3	8.04	28.11
	0.95	0.03	4	5.1	0.15	9.4	3.8	9.08	36.1

Table 14: Values selected from references are peak cross sections, and the four values in the last row are the cross sections obtained in the present work at $\sqrt{s} = 11$ GeV and $T = 0$ GeV. The cross sections are in units of mb.

Reference	$\pi J/\psi$	$\rho J/\psi$	$K J/\psi$	$K^* J/\psi$
[5]	2.5	0.9		
[6]	3.7	2.9		
[7]	6.2	3		
[10]			1.56	
[11]	0.83			
[12]	3.8			
[13]	7	2.7		
[14]	0.5	1.7	0.36	1.2
[16]	7			
[17]	0.9	5.7	0.8	
[18]	1.41	10.4		
[19]	0.37	2.12		
[20]			0.6	
[21]				1.05
	0.82	1.28	0.76	1.11